

1 **New U-Pb age constraints for the Laxford Shear Zone, NW Scotland:**
2 **Evidence for tectono-magmatic processes associated with the formation of**
3 **a Paleoproterozoic supercontinent.**

4 K.M. Goodenough^{1,*}, Q.G. Crowley^{2,3}, M. Krabbendam¹, and S.F. Parry⁴

5 1: British Geological Survey, West Mains Road, Edinburgh EH9 3LA, UK

6 2: NERC Isotope Geosciences Laboratory, Keyworth, Nottingham, NG12 5GG, UK

7 3: Department of Geology, School of Natural Sciences, Trinity College, Dublin 2, Ireland

8 4: British Geological Survey, Keyworth, Nottingham, NG12 5GG, UK

9 * Corresponding author: kmgo@bgs.ac.uk, +44 131 6500272

10

11 **Abstract**

12 The Lewisian Gneiss Complex in north-west Scotland is a part of the extensive network of
13 Archaean cratonic areas around the margins of the North Atlantic. It is considered to be made
14 up of a number of terranes with differing protolith ages, which have been affected by a range
15 of different metamorphic events. A major shear zone, the Laxford Shear Zone, forms the
16 boundary between two of these terranes. New dates presented here allow us to constrain the
17 timing of terrane assembly, related to the formation of Palaeoproterozoic supercontinents.
18 Early deformation along the Laxford Shear Zone, and primary accretion of the two terranes,
19 occurred during the Inverian event at c. 2480 Ma. This was followed by extension and the
20 intrusion of the mafic Scourie Dykes. Subsequently, renewed silicic magmatic activity
21 occurred at c. 1880 Ma, producing major granite sheets, considered to have formed as part of
22 a continental arc. A further collisional event began at c. 1790 Ma and was followed by slow

23 exhumation and cooling. This Laxfordian event caused widespread crustal melting,
24 metamorphism and deformation, and is considered to represent the final assembly of the
25 Lewisian Gneiss Complex within the major supercontinent of Columbia (or Nuna).

26

27 **Keywords**

28 Lewisian Gneiss Complex; Laxfordian; shear zone; geochronology

29

30 **1 Introduction**

31 The Lewisian Gneiss Complex of north-west Scotland is a fragment of Archaean crust,
32 variably reworked during the Proterozoic. The bulk of its outcrop lies within the foreland to
33 the Caledonian Orogen, and has been largely unaffected by Phanerozoic deformation and
34 metamorphism. It is thus an easily-accessible, well-mapped area in which to study problems
35 of Precambrian crustal evolution.

36 The Lewisian Gneiss Complex outcrops across two main areas: the islands of the Outer
37 Hebrides, and a broad strip along the north-west coast of mainland Scotland (Figure 1). The
38 whole complex shares the same basic geological history, as established by Sutton and Watson
39 (1951). This history begins with the formation of voluminous tonalite-trondhjemite-
40 granodiorite (TTG) gneisses in a number of Archaean magmatic events, followed by
41 heterogeneous late-Archaean deformation and metamorphism. During the early
42 Palaeoproterozoic, a swarm of mafic dykes (the Scourie Dyke Swarm) was intruded into this
43 Archaean basement. Some parts of the Lewisian were subsequently affected by
44 Palaeoproterozoic reworking.

45 This history encompasses a complex sequence of metamorphic, magmatic and deformational
46 events that have affected different parts of the Lewisian Gneiss Complex. Early field work

47 showed that some areas of TTG gneisses contained pyroxene (granulite-facies gneisses)
48 whilst others were amphibole-bearing (amphibolite-facies gneisses). On the mainland, a
49 central district of granulite-facies gneisses was mapped out, flanked by northern and southern
50 districts of amphibolite-facies gneiss (Peach et al., 1907). It was subsequently suggested that
51 the entirety of the Lewisian Gneiss Complex had been affected by a granulite-facies
52 ('Scourian') event prior to the emplacement of the Scourie Dykes, whereas only some areas
53 had been affected by a post-Scourie Dyke, amphibolite-facies, 'Laxfordian' event (Sutton and
54 Watson, 1951). Subsequent work recognised an amphibolite-facies, pre-Scourie Dyke event
55 termed the 'Inverian' that formed localised shear zones (Evans, 1965). The early granulite-
56 facies event was renamed from 'Scourian' to 'Badcallian' by Park (1970), to avoid any
57 confusion in terminology. Modern interpretations of the Lewisian Gneiss Complex continue
58 to use this framework of 1) a pre-Scourie Dyke, granulite-facies Badcallian event; 2) a pre-
59 Scourie Dyke, amphibolite-facies Inverian event; and 3) a post-Scourie Dyke, amphibolite-
60 facies Laxfordian event - although the Laxfordian may be divisible into more than one
61 discrete episode, and granulite-facies metamorphism may have occurred at different times in
62 different terranes (Kinny et al., 2005).

63 Bowes (1962, 1968) proposed that the Badcallian event may not have affected the whole of
64 the Lewisian Gneiss Complex. This view was not widely accepted, and at the time the
65 Lewisian was generally viewed as a single block of crust which had been affected by the
66 same tectonic events – albeit with juxtaposition of different crustal levels along shear zones
67 to create the heterogeneous patterns of metamorphism and deformation (Park and Tarney,
68 1987).

69 As modern geochronological techniques began to be applied during the 1980s and 1990s, it
70 became clear that the Lewisian gneisses were not all derived from protoliths of the same age
71 (Whitehouse, 1989, Kinny and Friend, 1997). This led to the development of a terrane model,

72 in which the Lewisian Gneiss Complex is considered to be made up of several different
73 crustal blocks that had different histories up until the point when they were juxtaposed into
74 their present relative positions (Friend and Kinny, 2001, Kinny et al., 2005). This concept is
75 now broadly accepted, although debate continues about the number of component terranes,
76 the position of their boundaries, and the nature and timing of their accretion (Mason and
77 Brewer, 2005, Park, 2005, Goodenough et al., 2010, Love et al., 2010).

78 One of the best candidates for a terrane boundary in the Lewisian is the Laxford Shear Zone,
79 in the northern part of the mainland outcrop. This paper presents new U-Pb geochronological
80 data for rocks from this shear zone, and provides new information about the timing of terrane
81 accretion in the north of the Lewisian Gneiss Complex. Two separate Palaeoproterozoic
82 magmatic events are recognised, and can be correlated with widespread activity across a
83 Palaeoproterozoic supercontinent.

84 **2 The geology of the Laxford Shear Zone**

85 The Laxford Shear Zone (LSZ) runs through Loch Laxford, in the mainland outcrop of the
86 Lewisian Gneiss Complex (Figure 1). It is a major polyphase shear zone, some 8 km wide
87 and WNW-trending (Coward, 1990), which separates amphibolite-facies gneisses to the north
88 from granulite-facies gneisses to the south. The northern, amphibolite-facies district has been
89 termed the Rhiconich terrane, whilst the central granulite-facies district, south of the LSZ, has
90 been named the Assynt terrane (Friend and Kinny, 2001). The field relationships around the
91 LSZ have been described in detail elsewhere (Goodenough et al., 2010) and are briefly
92 summarised here.

93 The lithologies to the south of the Laxford Shear Zone, around Scourie (Figure 2), are
94 banded, grey, pyroxene-bearing TTG gneisses of the Assynt terrane, with mafic to ultramafic
95 lenses and larger masses varying from a few cm to 100s of metres in size. The gneissic

96 banding generally dips gently towards the WNW. Locally, the gneisses and mafic-ultramafic
97 bodies are cut by thin (5 cm – 5 m) coarse-grained to pegmatitic granitoid sheets that are
98 foliated, but cut the gneissic banding (Evans and Lambert, 1974, Rollinson and Windley,
99 1980). All these lithologies are cut by NW-SE trending Scourie Dykes, typically 5-50 m
100 wide. The area is transected by discrete east-west amphibolite-facies shear zones, generally a
101 few metres wide, which deform and offset the dykes and are thus demonstrably Laxfordian in
102 age. Approaching the LSZ, these shear zones increase in abundance and swing into a NW-SE
103 orientation.

104 The southern margin of the LSZ is marked by the incoming of a steeply SW-dipping (50°-
105 70°), pervasive foliation in the gneisses, which has been formed by the thinning of the
106 original gneissic banding. This foliation is axial planar to folds of the gneissic banding, and
107 those folds are cross-cut by Scourie Dykes (Beach et al., 1974). The foliation is thus
108 considered to be Inverian in age, and to represent the first stage of deformation in the Laxford
109 Shear Zone. Discrete Laxfordian shear zones, generally less than 100 m in width, are
110 superimposed upon this Inverian structure. They are usually only identified where they cut
111 Scourie Dykes, which post-date the Inverian deformation, but were deformed during the
112 Laxfordian.

113 Within the LSZ lies a 1-2 km thick zone dominated by mafic-ultramafic lithologies ('early
114 mafic gneisses'), associated with brown-weathering, garnet-biotite semi-pelitic schists that
115 are considered to be metasedimentary in origin (Davies, 1974, Davies, 1976). These were
116 metamorphosed and deformed during both the Badcallian and Inverian events, as were
117 metasedimentary gneisses in a similar structural setting at Stoer, further south in the Assynt
118 terrane, (Zirkler et al., 2012). The zone of early mafic and metasedimentary gneisses in the
119 LSZ extends for some 15 km, from the coast on the SW side of Loch Laxford in the west to
120 Ben Stack in the east (Figure 2). Many of the mafic rocks are garnet-bearing amphibolites,

121 some of which contain relict granulite-facies assemblages and evidence for Badcallian partial
122 melting (Johnson et al., 2012), and they were deformed and foliated during the Inverian event
123 (Davies, 1974). The mafic-ultramafic-metasedimentary association is considered to be part of
124 the Assynt terrane, but its original relationship with the surrounding TTG gneisses is not
125 clear. This belt is cross-cut by Scourie Dykes, and also by scattered sheets of unfoliated
126 granite and granitic pegmatite that formed during the Laxfordian event (Goodenough et al.,
127 2010). Discrete Laxfordian shear zones are common in this area, but again are only easily
128 recognised where they affect Scourie Dykes.

129 To the north of the belt of mafic rocks, the grey TTG gneisses of the Assynt terrane rapidly
130 give way to migmatitic, granodioritic gneisses with abundant sheets and veins of granite and
131 granitic pegmatite. These migmatitic gneisses belong to the Rhiconich terrane. Within this
132 area, Scourie Dykes are folded, foliated and cross-cut by the granitic sheets (Goodenough et
133 al., 2010). The main magmatic and deformational event in these migmatitic gneisses is thus
134 considered to be Laxfordian in age, but the Laxfordian fabric is essentially parallel to – and
135 superimposed upon – the Inverian foliation in the southern part of the LSZ.

136 The boundary between the two terranes is rather variable in character along its length and can
137 be difficult to identify (Goodenough et al., 2010). In some areas it appears to be sharp, with
138 mafic-ultramafic rocks in the Assynt terrane being separated by a narrow, discrete shear zone
139 from migmatitic gneisses of the Rhiconich terrane; in other places, it lies within the felsic
140 gneisses, and is thus difficult to locate. East of Loch Laxford, this boundary is obscured by
141 thick (up to 100 m) weakly foliated granitic sheets, which cross-cut the gneissic banding at a
142 low angle.

143 The northern margin of the Laxford Shear Zone has generally been placed around Laxford
144 Bridge (Figure 2; Beach et al., 1974), but no sharp boundary exists, and Coward (1990) has
145 described the area north of Laxford Bridge as ‘a gently dipping Laxfordian shear zone’. In

146 summary, the LSZ can be considered as an Inverian shear zone marking the line of
147 juxtaposition of the Assynt and Rhiconich terranes. It was reactivated during the Laxfordian,
148 when the more hydrous, fusible gneisses of the Rhiconich terrane partially melted and were
149 pervasively deformed, whilst the brittle, dry gneisses of the Assynt terrane were only
150 deformed along discrete shear zones (Goodenough et al., 2010).

151 **3 Previous geochronological work**

152 The rocks of the Lewisian Gneiss Complex around the Laxford Shear Zone have been the
153 subject of a number of geochronological studies, the majority of which have focused on the
154 protolith and metamorphic ages of the TTG gneisses. The earliest work made use of the Rb-
155 Sr and K-Ar chronometers (Holmes et al., 1955, Giletti et al., 1961). Pegmatites from within
156 the Assynt terrane, which are cut by Scourie Dykes, were dated ‘as at least 2460 Ma’, whilst
157 the Laxfordian metamorphism was placed at ‘about 1600 Ma’ (Giletti et al., 1961). These
158 early radiometric age constraints were remarkably accurate for the time, and thus the broad
159 chronology of the Lewisian gneisses has been known for some 50 years.

160 Early Pb-Pb isotope work was interpreted to show that U depletion in the gneisses had
161 occurred at around 2900 Ma, and was assumed to be related to the Badcallian metamorphism
162 (Moorbath et al., 1969). Subsequent work with Sm-Nd isotopes refined this to give protolith
163 ages for the Lewisian gneisses of around 2950 Ma (Hamilton et al., 1979, Whitehouse and
164 Moorbath, 1986), whilst the Badcallian metamorphism was dated at 2660 to 2700 Ma using
165 U-Pb in zircon (Pidgeon and Bowes, 1972, Chapman and Moorbath, 1977, Cohen et al.,
166 1991). The Scourie Dykes were dated at 2000-2400 Ma using U-Pb techniques on
167 baddeleyite (Heaman and Tarney, 1989). Rb-Sr and K-Ar dating of samples from the Laxford
168 Shear Zone indicated that the ‘climax’ of the Laxfordian metamorphism occurred at
169 approximately 1850 Ma (Lambert and Holland, 1972), followed by relatively slow cooling.

170 Until the 1990s, it was considered that these dates could be extrapolated across the whole of
171 the Lewisian Gneiss Complex.

172 The development of high-precision U-Pb techniques for dating accessory minerals such as
173 zircon, and the ability to date individual crystals, or domains within crystals, revolutionised
174 dating of the Lewisian Gneiss Complex and revealed a level of chronological detail that
175 matches the complexity of observed field relationships. Protolith ages of TTG gneisses in the
176 Assynt terrane were shown to be c. 2960 Ma (Friend and Kinny, 1995), whilst gneisses in the
177 Rhiconich terrane have yielded younger protolith ages of c. 2840-2800 Ma and also record
178 magmatism at 2680 Ma (Kinny and Friend, 1997). Two high-grade metamorphic events were
179 recognised in gneisses of the Assynt terrane, the first at c. 2760 Ma (Corfu et al., 1994, Zhu et
180 al., 1997), and the second at c. 2490-2480 Ma (Whitehouse and Kemp, 2010, Corfu et al.,
181 1994, Friend and Kinny, 1995, Kinny and Friend, 1997)). These two metamorphic events
182 were correlated with the Badcallian and Inverian, respectively, by Corfu et al. (1994). Neither
183 event was recognised in zircon from the Rhiconich terrane gneisses (Kinny and Friend,
184 1997). Dating of titanites and monazites provided an age of c. 1750 Ma for the Laxfordian
185 metamorphism in both the Assynt and Rhiconich terranes, with a later phase of hydrothermal
186 activity at c. 1690-1670 Ma (Corfu et al., 1994; Zhu et al., 1997; Kinny and Friend, 1997).

187 The evidence for different protolith ages to the north and south of the Laxford Shear Zone,
188 together with the apparent lack of high-grade metamorphic events recorded in the Rhiconich
189 terrane, led Kinny and Friend (1997) to propose that the two blocks were in fact separate
190 terranes. They were considered to have had separate histories until their juxtaposition during
191 the Laxfordian event. Friend and Kinny (2001) suggested that Laxfordian granitic sheets are
192 only found in the Rhiconich terrane. They dated one of these sheets at c. 1854 Ma, and thus
193 proposed that the juxtaposition of the two terranes occurred after that date. However,
194 Goodenough et al. (2010) showed that the granitic sheets in fact 'stitch' the Laxford Shear

195 Zone, and are found within the Assynt terrane. The Laxford Shear Zone, which marks the
196 terrane boundary, is a major Inverian shear zone upon which Laxfordian shearing has been
197 superimposed, and thus the field relationships indicate that the terranes were juxtaposed
198 during the Inverian event (Goodenough et al., 2010).

199 The absolute age of the Inverian event remains a matter of debate. This event is defined on
200 the basis of field relationships as the amphibolite-facies metamorphism and deformation
201 which post-dates the granulite-facies metamorphism in the Assynt terrane, but pre-dates the
202 Scourie Dykes (Evans, 1965; Evans and Lambert, 1974). It is not recognisable in the field in
203 the Rhiconich terrane, but this may be due to the intensity of later Laxfordian deformation. A
204 suite of pegmatites found in the Lochinver and Scourie areas is unaffected by Badcallian
205 deformation and metamorphism, but is deformed in Inverian shear zones, and has generally
206 been considered to have formed at an early stage in the Inverian event (Evans and Lambert,
207 1974, Tarney and Weaver, 1987, Corfu et al., 1994). These pegmatites have been dated at c.
208 2480 Ma (Corfu et al., 1994; Zhu et al., 1997). Although interpretation of Lewisian zircon is
209 certainly not straightforward, many authors have placed the Badcallian high-grade
210 metamorphic event at c. 2700 – 2800 Ma, which would fit with an Inverian event at c. 2480
211 Ma (Corfu et al., 1994; Zhu et al., 1997; Whitehouse and Kemp, 2010). An alternative view
212 suggests that high-grade metamorphism affected the Assynt terrane at c. 2490 - 2480 Ma and
213 that this equates to the Badcallian (Love et al., 2004, Kinny et al., 2005), which would place
214 the Inverian in the interval between c. 2480 Ma and the oldest Scourie Dyke at c. 2400 Ma
215 (Heaman and Tarney, 1989).

216 Recent detailed mapping of the Laxford Shear Zone has allowed clear identification of
217 structures and intrusions formed during the Inverian and Laxfordian events (Goodenough et
218 al., 2010). Samples from well-characterised outcrops were collected for radiometric dating, in

219 order to constrain the timing of the Inverian and Laxfordian events, and their related
220 magmatism. The sample localities are indicated on Figure 2, and briefly described below.

221 **4 Sample localities**

222 *4.1 Badnabay*

223 The belt of mafic-ultramafic and metasedimentary gneisses, which forms the northern margin
224 of the Assynt terrane, is well exposed around 1 km south of Badnabay, on the south side of
225 Loch Laxford. The gneisses around Badnabay itself are migmatitic quartzofeldspathic
226 gneisses, containing abundant granitic veins and sheets, and belong to the Rhiconich terrane.
227 To the south, these pass into well-banded hornblende-bearing tonalitic gneisses of the Assynt
228 terrane, although a sharp contact cannot be mapped out between the two gneiss types. Around
229 [NC 216 457], the tonalitic gneisses are in contact with brown-weathering garnet-biotite
230 schists and coarse-grained garnet amphibolite, which belong to the main mafic-ultramafic-
231 metasedimentary belt. The garnet amphibolites of this belt locally contain remnant two-
232 pyroxene assemblages and evidence for partial melting, and so the belt is considered to have
233 been metamorphosed to granulite facies during the Badcallian (Johnson et al., 2012). All the
234 lithologies carry a strong NW-SE-trending, steeply-dipping foliation and an ESE-plunging
235 lineation. These structures are cut by Scourie Dykes along strike, and are thus attributed to
236 the Inverian. The metasedimentary rocks and tonalitic gneisses are cut by an irregular,
237 anastomosing coarse-grained granitic sheet, 1-5 m thick, which is undeformed. This
238 represents one of the most southerly Laxfordian granites within the Assynt terrane.

239 Sample LX1 was collected from the granite sheet at [NC 21679 45741]. It is a medium- to
240 coarse-grained, fairly equigranular, two-feldspar biotite-muscovite granite. Sample LX2 was
241 collected from the metasedimentary biotite schists at [NC 21638 45754]. It is a medium-

242 grained, strongly recrystallised garnetiferous semi-pelite, comprising quartz, plagioclase,
243 biotite and garnet.

244 *4.2 Tarbet*

245 The traverse from the coastal village of Tarbet to Rubha Ruadh on the south shore of Loch
246 Laxford is considered to be the classic section through the Laxford Shear Zone (Beach,
247 1978). At [NC 16379 49320], hornblendic mafic gneisses of the Assynt terrane are cut by
248 numerous thin (up to 50 cm), pink microgranitic sheets. Both gneisses and microgranitic
249 sheets carry a strong NW-SE trending, steeply dipping foliation and are folded into tight
250 upright folds that are axial planar to the foliation (Figure 3a). The foliation is considered to be
251 Inverian in age, on the basis of relationships with Scourie Dykes along strike. It is possible
252 that a component of Laxfordian deformation has been superimposed on the main Inverian
253 fabric, but cannot be distinguished here. Some 15 m to the west, the Inverian foliation is
254 locally cross-cut by sheets of undeformed pink coarse-grained Laxfordian granite. Sample
255 LX11 was collected from a thin, folded, foliated microgranite sheet that was clearly affected
256 by Inverian deformation. The microgranite is medium-grained, with a foliation defined by
257 ribbons of recrystallised quartz separated by zones of sericitised alkali feldspar + quartz +
258 muscovite + biotite.

259 *4.3 Ben Stack*

260 On the north side of Ben Stack, thick (up to 100 m) sheets of foliated, medium- to coarse-
261 grained granite are intruded along the boundary between the Assynt and Rhiconich terranes.
262 On a map scale, these granite sheets cross-cut the Inverian foliation, but they were themselves
263 weakly deformed during the Laxfordian event. They contain relatively small amounts (~ 15%
264 of the rock) of mafic minerals that include alkali amphibole and alkali pyroxene. Mineral
265 phases such as these are unlikely to have crystallised from the peraluminous melts that would

266 be derived by melting of the local crust alone (Watkins et al., 2007). These granite sheets
267 therefore represent the addition of at least a component of juvenile magma to the crust.
268 Sample LX6 was collected from one of these thick granite sheets at [NC 26050 43696]. It is a
269 medium- to coarse-grained, equigranular granite with a weak foliation defined by aligned
270 mafic mineral phases. The mineralogy comprises quartz, alkali feldspar, plagioclase, aegirine,
271 and an alkali amphibole, with abundant accessory titanite as well as zircon and monazite. The
272 granite has been recrystallised and foliated after emplacement, but with little or no new
273 mineral growth, although titanites show evidence of some alteration and late overgrowths.

274 *4.4 Rhiconich*

275 Around the village of Rhiconich, migmatitic gneisses typical of the Rhiconich terrane are
276 exposed. These gneisses are intruded by abundant, irregular, undeformed granitic sheets and
277 pegmatites that cross-cut the banding in the gneisses (Figure 3b). The main mafic minerals in
278 these granites are chlorite and muscovite, and field relations indicate that these granites may
279 have been largely derived by melting of local crust, although experimental data suggest that
280 an additional component of melt may have been required to produce the more potassic
281 granites (Watkins et al., 2007). Foliated amphibolites in this area, which are considered to be
282 members of the Scourie Dyke Swarm, are also cut by the granitic sheets. The pervasive
283 deformation of these Scourie Dykes indicates that the whole area was affected by Laxfordian
284 deformation. In contrast, the granitic sheets are undeformed, and therefore were intruded at a
285 relatively late stage in the Laxfordian event. Sample LX7 was collected from one such
286 granitic pegmatite sheet in a road cutting at [NC 24645 51912]. The sample is very coarse-
287 grained, being largely made up of quartz and alkali feldspar with abundant evidence of
288 recrystallisation along grain boundaries. Chlorite (after biotite) and muscovite form <10% of
289 the rock.

290

291 **5 Methodology and analysis**

292 Individual samples of approximately 5 kg of fresh, unaltered material were crushed and
293 sieved using standard mineral preparation procedures. Heavy minerals were concentrated
294 using a Wilfley table prior to gravity settling through methylene iodide for separation of the
295 heavy mineral concentrate, which was subsequently washed in acetone and dried. Zircons,
296 titanites and monazites were separated initially by paramagnetic behaviour using a Franz
297 isodynamic separator and then hand-picked from the non-magnetic and least magnetic
298 fractions.

299 *5.1 Laser-ablation Multicollector Inductively Coupled Plasma Mass Spectrometry (LA-MC-*
300 *ICP-MS)*

301 LA-MC-ICP-MS U-Pb geochronology was performed at the NERC Isotope Geosciences
302 Laboratory (UK). Mineral separates were mounted in an araldite resin block, ground to near
303 mid-thickness and polished. Cathodoluminescence (CL) images of zircon grains (Figure 4)
304 were acquired at the British Geological Survey using an FEI QUANTA 600 Environmental
305 Scanning Electron Microscope (tetrode tungsten gun version) equipped with a KE
306 Developments Centaurus Cathodoluminescence Detector, and these were used to select target
307 spots for analysis. Analyses used a Nu Plasma MC-ICP-MS system coupled to a New Wave
308 Research 193nm Nd:YAG LA system. A laser spot size of 25 microns was used to ablate
309 discrete zones within grains. The total acquisition cycle was about one minute, which
310 equates to approximately 15µm depth ablation pits. A $^{205}\text{Tl}/^{235}\text{U}$ solution was simultaneously
311 aspirated during analysis using a Cetac Technologies Aridus desolvating nebulizer to correct
312 for instrumental mass bias and plasma induced inter-element fractionation. Data were
313 collected using static mode acquiring ^{207}Pb , ^{206}Pb and ^{204}Pb &Hg in ion counting detectors. A
314 common-Pb correction based on the measurement of ^{204}Pb was attempted, but interference
315 from the ^{204}Hg peak overwhelmed the common-Pb contribution from the zircon grains. As a

316 result of this, data presented are non-common Pb corrected. Analyses with high common Pb
317 (^{204}Pb cps in excess of 200cps) were rejected, but these amounted to a <0.5% of the total data
318 set and were not disproportionately from any one sample. Some minor elevation in common
319 Pb may be responsible for generating excess scatter in the calculated weighted mean
320 $^{207}\text{Pb}/^{206}\text{Pb}$ ages. Data were normalised using the zircon standard 91500 whereas two
321 additional zircon standards (GJ-1 and Mud Tank) were treated as unknown samples to
322 monitor accuracy and precision of age determinations. During the various analytical sessions
323 secondary standards produced values within error of published ages. GJ-1 gave a Concordia
324 age of 607.1 ± 2.7 Ma (reported TIMS $^{207}\text{Pb}/^{206}\text{Pb}$ is 608.5 ± 0.4 Ma (Jackson et al., 2004)),
325 and Mud Tank gave a Concordia age of 733.3 ± 3.7 Ma (TIMS age 732 ± 5 Ma (Black and
326 Gulson, 1978)). Raw measured intensities of ^{204}Pb for these secondary standards did not
327 deviate significantly from those of the unknowns, indicating that the treatment of non-
328 common Pb data produces ages within error of TIMS common-Pb corrected data. Data were
329 reduced and errors propagated using an in-house spreadsheet calculation package, with ages
330 determined using the Isoplot 3 macro of Ludwig (2003). Uncertainties for each ratio are
331 propagated relative to the respective reproducibility of the standard, to take into account the
332 errors associated with the normalisation process and additionally to allow for variations in
333 reproducibility according to count rate of the less abundant ^{207}Pb peak. All ages are reported
334 at the 2σ level. A full description of analytical protocols can be found in Thomas et al.
335 (2010). Data are presented in tables 1 and 3-7.

336

337 *5.2 Thermal Ionization Mass Spectrometry (TIMS)*

338 Dating of selected samples was conducted by isotope dilution thermal ionization mass
339 spectrometry (ID-TIMS) in order to produce higher precision data and to provide independent
340 verification of LA-MC-ICP-MS data. Zircon was thermally annealed and leached by a

341 process modified from that of Mattinson (Mattinson, 2005). Zircon grains from individual
342 samples were annealed as bulk fractions at 850°C in quartz glass beakers for 60 hours. Once
343 cooled, the zircon grains were ultrasonically washed in 4N HNO₃, rinsed in ultra-pure water,
344 then further washed in warm 4N HNO₃ prior to rinsing with water to remove surface
345 contamination. The annealed and cleaned zircon fractions were then chemically leached in
346 Teflon microcapsules enclosed in a Parr bomb using 200µl 29N HF and 20µl 8N HNO₃ at
347 180°C for 12 hours to minimise or eliminate damaged zones in which Pb loss may have
348 occurred. TIMS data are presented in table 2.

349 A mixed ²⁰⁵Pb – ²³³U – ²³⁵U EARTHTIME tracer was used to spike all fractions, which once
350 fully dissolved, were converted to chloride and loaded onto degassed rhenium filaments in
351 silica gel, following a procedure modified after Mundil et al. (2004). A Thermo Electron
352 Triton at NIGL was used to collect all U-Pb TIMS data. Approximately 100 to 150 ratios of
353 Pb isotopic data were dynamically collected using a MassCom Secondary Electron Multiplier
354 (SEM). Between 60 and 80 ratios were statically collected using either a SEM or Faraday
355 cups for U, depending on signal strength. Pb ratios were scrutinised for any evidence of
356 organic interferences using an in-house raw ratio statistical and plotting software, but these
357 were found to be negligible or non-existent. Errors were calculated using numerical error
358 propagation (Ludwig, 1980). Isotope ratios were plotted using Isoplot version 3.63 (Ludwig,
359 1993, Ludwig, 2003); error ellipses on concordia diagrams reflect 2σ uncertainty. Total
360 procedural blanks were 1.0 pg for Pb and c. 0.1 for U. Samples were blank corrected using
361 the measured blank composition. Correction for residual common lead above analytical
362 blank was carried out using the Stacey-Kramers common lead evolutionary model (Stacey
363 and Kramer, 1975).

364

365 **6 Results**

366 6.1 *Badnabay*

367 Two distinct morphological types of zircon were separated from sample LX1, the
368 undeformed granite cutting mafic gneisses and metasedimentary rocks within the Laxford
369 Shear Zone. Small, acicular zircon grains (c. 80x30x20 μm), interpreted as igneous in origin
370 using CL imaging, were dated using ID-TIMS. Three single grain fractions form a cluster on
371 concordia with a mean $^{207}\text{Pb}/^{206}\text{Pb}$ age of $1773.1 \pm 1.1\text{Ma}$ (Figure 5a). One discordant
372 fraction shows evidence of Pb-loss evidently not removed by the chemical abrasion
373 procedure. Larger (c. 150x120x120 μm), multi-faceted zircon grains from the same sample
374 (Figure 4) were dated using LA-ICPMS. Overgrowths identified in CL images and
375 interpreted as igneous in origin give a mean $^{207}\text{Pb}/^{206}\text{Pb}$ age of $1774 \pm 5.6\text{Ma}$ (Figure 5b),
376 within error of the ID-TIMS age on acicular zircon from the same sample. Analyses of
377 inherited cores from multi-faceted zircon give a range of ages, in excess of c. 2558 Ma. The
378 ID-TIMS age of $1773.1 \pm 1.1\text{Ma}$ is taken as the best estimate for the intrusive age of this
379 granite sheet.

380 Zircon from the metasedimentary biotite schist, sample LX2, was dated using LA-ICPMS.
381 Zircon grains from this sample vary from c. 300x150x150 to 150x100x100 μm , typically
382 with ovoid morphologies characteristic of detrital grains. CL images of these grains reveal
383 subtle metamorphic textures such as net-veining and patchy growth zonation (Figure 4). The
384 analyses give a range of ages from c. 2475 Ma to 2784 Ma (Figure 5c). Although there is a
385 cluster of analyses at c. 2685 Ma, it is not possible to recognise statistically coherent age
386 groups within the dataset, as the analyses plot along concordia within the age range. The ages
387 determined for this sample are not considered to represent true detrital ages, but are
388 interpreted to have been affected by partial resetting due to granulite-facies metamorphism
389 and/ or Pb-loss, and therefore cannot be used to infer a maximum depositional age for the
390 original sedimentary rocks. This interpretation of metamorphic resetting is consistent with the

391 relict granulite-facies mineral assemblage and evidence for partial melting in the associated
392 mafic-ultramafic rocks (Johnson et al., 2012), and field evidence for deformation and
393 metamorphism during the Inverian event. The youngest ages (c. 2475 Ma) are considered to
394 approximate to the timing of the Inverian event, after which the zircon systematics were not
395 disturbed.

396 *6.2 Tarbet*

397 Zircon grains from sample LX11, the folded and foliated microgranite, are typically c.
398 400x200x200 to 250x150x100 μm . They have abundant, large igneous oscillatory zoned
399 cores with igneous oscillatory zoned overgrowth patterns of variable width, and narrow (2-30
400 μm), bright CL rims (Figure 4). The latter are consistent with a metamorphic origin or some
401 disturbance of the zircon lattice structure due to deformation assisted fluid infiltration. The
402 majority of analyses from this sample are slightly discordant (1-6%) (Figure 5d). A discordia
403 through 54 out of the total of 69 analyses for this sample (15 analyses were excluded for
404 lying off the main discordia trajectory) yields an upper-intercept age of 2843 ± 33 Ma and a
405 lower-intercept age of c. 1750 Ma (Figure 5d). Note that only one analysis lies close to c.
406 1750 Ma, hence the poorly constrained lower-intercept age. A number of analyses (n=11) lie
407 on a mixing chord between c. 2480 Ma and >2850 Ma, suggesting that a c. 2480 Ma event
408 also affected the zircon from this sample. Given the width of the bright CL rims, it was
409 difficult to avoid ablating a mixture of rim and igneous zircon, so a number of analyses
410 represent a mixture of older igneous growth (possibly both c. 2843 and c. 2480 Ma) and
411 younger rims (c. 1750 Ma). It is difficult to place an unequivocal interpretation on these
412 complex data, but we suggest that the c. 2843 Ma age represents the protolith age of the
413 country rock gneisses, which were subsequently partially melted to form the granite sheets
414 during metamorphism and deformation at c. 2480 Ma, with subsequent metamorphism at c.
415 1750 Ma.

416 6.3 Ben Stack

417 Zircon and titanite were recovered from sample LX6, taken from the thick granite sheet on
418 the north side of Ben Stack. Zircon grains typically are 300x250x200 to 200x100x100 μm ,
419 with some oscillatory zonation evident in CL. Patchy, dull and net-veined CL patterns and
420 obvious inherited cores also exist in many zircon grains from this sample (Figure 4). Titanite
421 grains are large, up to 1 mm in length, with some evidence of alteration and late overgrowths.
422 Both zircon and titanite were dated by LA-ICPMS. U-Pb zircon analyses plot along
423 concordia, mainly between c. 1880 and 2765 Ma (Figure 6a). A frequency probability plot of
424 all the zircon LA-ICPMS data for LX6 shows a dominant peak at c. 1880 Ma, with a
425 subordinate peak at c. 2480 to 2500 Ma (Figure 6b). A weighted mean $^{207}\text{Pb}/^{206}\text{Pb}$ age of the
426 main population gives 1880.1 ± 4.2 Ma (Figure 6c). Apparent ages intermediate between c.
427 2765-2500 Ma and 1883-2480 Ma are most likely analytical artefacts of mixing by ablating
428 different age domains. The age of 1880.1 ± 4.2 Ma is taken as the best estimate for
429 emplacement of this granite body, with older ages representing abundant inherited grains.

430 Titanite analyses have variable amounts of common Pb. When all titanite LA-ICPMS
431 analyses are plotted on a Tera Wasserburg diagram, they fall along a discordia with a lower
432 intercept at $1671 + 12/ -11$ Ma (Figure 6d). It is possible that there are two separate
433 trajectories on this diagram, indicating that there may be more than one titanite age present in
434 this sample, but this is not resolvable as the analyses are within analytical uncertainty. The
435 age of $1671 + 12/ -11$ Ma is considered to be a cooling age for titanite.

436 6.4 Rhiconich

437 Zircon from sample LX7, the granite sheet from the Rhiconich terrane, was dated using LA-
438 ICPMS. Zircon grains are typically 400x200x150 to 150x75x50 μm with abundant inherited
439 cores visible in CL images (Figure 4). A concordia diagram (Figure 6e) shows a cluster of

440 analyses at c. 1790 Ma and older ages between c. 2550 and 2860 Ma. A weighted mean
441 $^{207}\text{Pb}/^{206}\text{Pb}$ age of the four least discordant analyses from the younger main age population
442 gives 1792.9 ± 3.0 Ma, (Figure 6f) which is taken as the best estimate of the intrusion age of
443 the granite. The older dates between c. 2550 and 2860 Ma are interpreted as inherited ages.
444 Two analyses at c. 1980 and 2360 Ma are discordant, and most probably represent mixtures
445 of c. 1790 and > 2500 Ma components.

446

447 **7 Discussion**

448 *7.1 Archaean to earliest Palaeoproterozoic events*

449 Dating of individual metamorphic events within the Lewisian Gneiss Complex has generally
450 proved problematic (e.g. Corfu et al., 1994; Kinny et al., 2005; Whitehouse and Kemp, 2010),
451 as it is generally difficult to clearly relate new zircon growth to either Badcallian or Inverian
452 metamorphism; there is no definitive textural test to distinguish between amphibolite-facies
453 and granulite-facies zircon. However, two samples in this study, the deformed granite from
454 Tarbet (LX11) and the metasedimentary rock from Badnabay (LX2), do show clear field
455 evidence for Inverian deformation.

456 Field relationships suggest that the thin, deformed microgranitic sheets near Tarbet were
457 probably formed by partial melting of local crustal material, and were intensely deformed and
458 recrystallised during the Inverian and possibly the Laxfordian events. CL images of zircon
459 from this sample show that igneous zircon, dated at 2843 ± 33 Ma, is volumetrically
460 dominant. Bright CL rims are present in zircon from this sample and two separate mixing
461 trajectories may exist, defining two separate lower-intercept ages of c. 2480 and c. 1750 Ma.
462 However, it is not possible to attribute these lower intercept ages to particular rim domains
463 visible in CL. Although this sample locality lies near the northern margin of the Assynt

464 terrane as defined in the field, the inherited protolith age of c. 2843 Ma is within error of
465 those observed for gneisses in the Rhiconich terrane (Kinny and Friend, 1997), and this
466 suggests that the terranes may share more magmatic events than previously thought. The data
467 are best explained by formation of the country rock gneisses at c. 2843 Ma, followed by a
468 metamorphic event at c. 2480 Ma during which partial melting generated the granitic sheets.
469 Metamorphism and deformation during a subsequent event at c. 1750 Ma caused growth of
470 thin rims and disturbance of U-Pb systematics.

471 The c. 2843 Ma protolith age for the country rock gneisses indicates magmatism within the
472 Assynt terrane at that time. The lower intercept ages, whilst not definitive, indicate a high-
473 temperature metamorphic event at c. 2480 Ma during which the granitic sheets were formed
474 by partial melting. Granitic sheets of this age are only recognised within the Inverian shear
475 zone, and so this event at c. 2480 Ma is most likely to be the Inverian as suggested by a
476 number of authors (Corfu et al., 1994; Zhu et al., 1997; Whitehouse and Kemp, 2010).

477 However, we cannot completely rule out the possibility that the granitic sheets were formed
478 in a Badcallian granulite-facies event at c. 2480 Ma which was immediately followed by the
479 Inverian deformation, and subsequently by a Laxfordian event at c. 1750 Ma.

480 The metasedimentary sample (LX2) from Badnabay contains zircon with a range of ages
481 which were likely reset by high-grade metamorphism, as demonstrated by metamorphic
482 textures evident in CL imaging and by the spread of analyses overlapping within uncertainty
483 with the concordia curve between c. 2475 and 2784 Ma. On this basis, they cannot be used to
484 provide information about the source of the original sedimentary rocks. The youngest ages
485 from this sample are c. 2475 Ma and we interpret this age as approximating the end of the
486 Inverian event. This age is within error of the lower intercept age of c. 2480 Ma for sample
487 LX11, and indicates that the age of Inverian high-grade metamorphism and deformation in
488 the Laxford Shear Zone was around 2480 Ma.

489 *7.2 Palaeoproterozoic events*

490 The term 'Laxfordian' has traditionally been used to describe all events in the Lewisian
491 Gneiss Complex that post-date the Scourie Dykes, but it is becoming clear that this
492 encompasses a whole range of metamorphic and magmatic events (Kinny et al., 2005). This
493 is exemplified by our new U-Pb data (Table 8). The thick foliated granite sheets on the north
494 side of Ben Stack are part of the Rubha Ruadh granite suite of Kinny et al. (2005). These
495 voluminous granites, which intrude the boundary zone between the Assynt and Rhiconich
496 terranes, are associated with an input of juvenile magma into the crust. The new emplacement
497 age of 1880.1 ± 4.2 Ma (sample LX6) is close to the 1854 ± 13 Ma date obtained by Friend
498 and Kinny (2001) from another intrusion in this suite, and our new date for sample LX6
499 significantly extends the duration of this magmatism.

500 Magmatism is known to have occurred elsewhere within the Lewisian Gneiss Complex at
501 roughly this time, notably in the South Harris Complex of the Outer Hebrides at c. 1890 Ma
502 (Mason et al., 2004), in the Nis terrane on the Isle of Lewis at c. 1860-1870 Ma (Whitehouse,
503 1990, Whitehouse and Bridgwater, 2001) and in the Loch Maree Group further south on the
504 mainland at c. 1900 Ma (Park et al., 2001). High-grade metamorphism of similar age has also
505 been recognised in the Ialltaig gneisses, further south in the mainland Lewisian Gneiss
506 Complex (Love et al. 2010), and in the gneisses of South Harris (Whitehouse and Bridgwater,
507 2001, Friend and Kinny, 2001, Mason, 2012). These ages are generally associated with the
508 development of magmatic arcs which were subsequently accreted and buried by continental
509 collision (Whitehouse and Bridgwater, 2001; Park et al., 2001).

510 A relatively thin, undeformed granite sheet, cutting the Assynt terrane within the Laxford
511 Shear Zone, has been dated at 1773.1 ± 1.1 Ma (sample LX1). A similar granitic sheet from
512 the Rhiconich terrane has been dated at c. 1793 Ma (sample LX7). Field relationships
513 indicate the likelihood that these granitic sheets were derived by local crustal melting,

514 potentially during an episode of crustal thickening. Although intrusions of this age have not
515 been recorded elsewhere in the Lewisian Gneiss Complex, formation of hydrothermal titanite
516 at >1754 Ma (Corfu et al., 1994) and resetting of earlier formed titanite at c. 1750 Ma (Corfu
517 et al., 1994, Kinny and Friend, 1997) have been recorded in both the Assynt and Rhiconich
518 terranes. Metamorphic rims from deformed granitic sheets in the Laxford Shear Zone also
519 give ages of c. 1750 Ma (sample LX11). U-Pb dating of titanites in the Ben Stack granitic
520 sheet, sample LX6, indicates that these rocks were cooled slowly from their peak
521 temperature, with the titanite cooling through its closure temperature (600-700°C) at c. 1670
522 Ma. This overlaps within error (1690-1670 Ma) with growth of secondary titanite and rutile
523 considered to be related to low grade alteration and hydrothermal growth of these minerals
524 (Corfu et al 1994). There is no evidence for secondary growth of titanite in sample LX6; the
525 dated titanites appear to be igneous in origin. Taken together, all these ages indicate a long-
526 lived crustal heating event, followed by slow cooling, in the northern part of the Lewisian
527 Gneiss Complex between c. 1790 and c. 1670 Ma – encompassing the events defined as
528 Laxfordian and Somerledian by Kinny et al. (2005). Somerledian ages have been recognised
529 throughout the Lewisian Gneiss Complex (Corfu et al., 1994; Love et al., 2004).

530 It seems that at least two main magmatic events affected much of the Lewisian Gneiss
531 Complex in the Palaeoproterozoic. The first involved formation of a magmatic arc and
532 introduction of mantle-derived magma in one or more pulses along the margins of the gneiss
533 terranes at c. 1900-1870 Ma. This was followed by a later crustal thickening, heating and
534 melting event which began at c. 1790 Ma and continued, cooling slowly, to c. 1660 Ma.
535 Evidence of these events cannot be used on its own to correlate different terranes or terrane
536 boundaries, since it is now clear that most terranes in the Lewisian Gneiss Complex were
537 affected by these Palaeoproterozoic events.

538 *7.3 Comparison with other North Atlantic cratonic areas*

539 The magmatism that occurred throughout much of the Lewisian Gneiss Complex at c. 1900-
540 1870 Ma and c. 1790 Ma can be related to the development of magmatic arcs and the
541 accretion of an ancient supercontinent (Columbia or Nuna; Zhao et al. (2004), Rogers and
542 Santosh (2002)). This supercontinent incorporated much of the existing crust at that time, and
543 therefore collisional belts of this age are widespread across the globe. Within the British Isles,
544 orthogneisses of similar age (1780 – 1880 Ma; Marcantonio et al. (1988), Daly et al. (1991),
545 McAteer et al. (2010)) are also found in the Rhinns Complex of western Scotland, which
546 extends south-westwards to Ireland.

547 In southwestern Greenland, along the southern margin of the Archaean craton, the Ketilidian
548 belt contains plutons emplaced in a continental magmatic arc that formed at c. 1854-1795 Ma
549 (Garde et al., 2002a). This was followed by uplift and deformation of the fore-arc at c. 1795-
550 1780 Ma with widespread anatexis and emplacement of S-type granites (Garde et al., 2002b).
551 Similarly, the Nagssugtoqidian orogen to the north of the Greenland Archaean craton
552 contains evidence for arc magmatism at 1940-1870 Ma followed by high-grade
553 metamorphism (Kalsbeek and Nutman, 1996, van Gool et al., 2002, Nutman et al., 2008)
554 with subsequent lower-grade metamorphism at c. 1780-1750 Ma. Palaeoproterozoic
555 accretionary belts of similar age extend westwards into North America, including the
556 Torngat, New Quebec and Trans-Hudson orogens (van Kranendonk et al., 1993, Scott, 1998,
557 St-Onge et al., 2009).

558 In Scandinavia, the Lapland-Kola Belt also contains juvenile, arc-type magmas of c. 2000-
559 1860 Ma (Daly et al., 2006) although here there is evidence for major crustal shortening and
560 high-grade metamorphism at c. 1950-1870 Ma, rather earlier than is recognised in Scotland.
561 The Svecofennian Orogen is a collage of Palaeoproterozoic, arc-type magmatic units
562 emplaced in two main pulses at 1900 – 1870 and 1830 – 1790 Ma (Lahtinen et al., 2009).

563 Overall, it is clear that Palaeoproterozoic events in the Lewisian Gneiss Complex can be
564 correlated with those in the surrounding cratonic areas.

565

566 **8 Refining the model for the Lewisian Gneiss Complex**

567 An overall model for the Lewisian Gneiss Complex has been discussed by many authors
568 (Park, 1995, Whitehouse and Bridgwater, 2001, Park, 2005, Kinny et al., 2005, Wheeler et
569 al., 2010). Our new data (summarised in Table 8) contribute to the understanding of this
570 evolution of the Lewisian, and hence of the Laurentian craton, through the Precambrian.

571 The TTG protoliths of the Lewisian Gneiss Complex originally formed within a number of
572 crustal fragments or terranes at varying times within the Archaean (Kinny and Friend, 1997;
573 Friend and Kinny, 2001; Kinny et al., 2005). Protolith ages within the Assynt terrane have
574 previously been described as 3030-2960 Ma (Kinny et al., 2005) but our data also provide
575 evidence for protoliths at c. 2843 Ma, an age more typically associated with the Rhiconich
576 terrane. This suggests that the different terranes may all contain magmatic protoliths of a
577 range of different ages.

578 Some of these terranes, most notably the Assynt terrane, underwent high-grade
579 metamorphism during the Badcallian event, which has been variously linked with recognised
580 dates for metamorphism at 2700-2800 Ma (Corfu et al., 1994; Whitehouse and Kemp, 2010)
581 or 2490-2480 Ma (Kinny and Friend, 1997, Kinny et al., 2005). The Badcallian event
582 produced granulite-facies metamorphic assemblages and crustal anatexis, but the driving
583 causes of this event are not known. Subsequently, parts of the Lewisian Gneiss Complex
584 were affected by the Inverian amphibolite-facies event with the formation of major shear
585 zones (Evans, 1965), possibly at c.2480 Ma (Corfu et al., 1994; Zhu et al., 1997). Our data
586 support a relatively high-temperature metamorphic event in the Laxford Shear Zone at c.

587 2480 Ma, which we link with the Inverian on the basis of relationships to Inverian structures.
588 This event is recognised in both the Assynt and Gruinard terranes (Kinny et al., 2005), and it
589 is likely that all the mainland Lewisian terranes to the north of Gairloch were assembled
590 together at this time (Goodenough et al., 2010), with development of the Laxford Shear Zone.
591 However, our data do not provide further constraints for the timing of the Badcallian event.

592 During the early part of the Palaeoproterozoic, the Lewisian Gneiss Complex largely lay
593 within an extending continent, marked by the emplacement of the Scourie Dyke Swarm. By
594 1900 Ma, active margins existed along the edge of many continental fragments, creating a
595 network of magmatic arcs which has been recognised across all the cratonic areas around the
596 North Atlantic. Juvenile magmas formed in this setting were emplaced along the continental
597 margin and within the Lewisian Gneiss Complex, where they followed the lines of weakness
598 created by older terrane boundaries such as the Laxford Shear Zone. Subsequent collision of
599 arc fragments led to localised high-temperature metamorphism in rocks associated with the
600 South Harris Complex and Loch Maree Group (Love et al., 2010; Mason, 2012). Further
601 north, many of the classic Laxfordian shear zones seen within the Assynt terrane are
602 considered to have formed during this event, since they are cross-cut by undeformed
603 granitoids emplaced at c. 1790-1770 Ma. This collisional event is considered to have been a
604 part of the accretion of a major supercontinent, Columbia (or Nuna).

605 The subsequent metamorphic event or events, which began at c. 1790 Ma and continued to c.
606 1670 Ma, is recognised throughout the Lewisian Gneiss Complex and considered to represent
607 the final assembly of all Lewisian terranes, particularly those in the southern part of the
608 complex (Love et al., 2010). During this event, much of the Lewisian crust was buried and
609 heated, with more fertile potassic gneisses such as those in the Rhiconich terrane melting to
610 produce granites and pegmatites. The anhydrous granulite-facies gneisses of the Assynt
611 terrane are relatively infertile (Watkins et al., 2007) and were not affected by melting.

612 Alteration and secondary growth of minerals such as monazite, titanite and rutile occurred in
613 many lithologies within the Lewisian Gneiss Complex at this time. After c. 1670 Ma, the
614 Lewisian Gneiss Complex became part of a stable craton, within a series of supercontinents.

615

616 **Acknowledgements**

617 This work is published with the permission of the Executive Director of the British
618 Geological Survey. John Mendum and John Macdonald are thanked for their constructive
619 comments on earlier versions of the paper. Constructive reviews by John Wheeler and
620 Fernando Corfu, and editorial advice from Randy Parrish, were much appreciated, and have
621 materially improved the paper. Dating work was funded through the BGS-NIGL funding
622 scheme. This is a contribution to IGCP-SIDA Project 599 (The Changing Early Earth).

623

624 **References**

625

- 626 Beach, A., Coward, M. P., Graham, R. H., 1974. An interpretation of the structural evolution of the
627 Laxford front. *Scottish Journal of Geology* 9, 297-308.
- 628 Black, L. P., Gulson, B. L., 1978. The age of the Mud Tank carbonatite, Strangways Range, Northern
629 Territory. *BMR Journal of Australian Geology and Geophysics* 3, 227-232.
- 630 Bowes, D. R., 1962. Untitled discussion. *Proceedings of the Geological Society of London* 1594, 28-
631 30.
- 632 Bowes, D. R. 1968. An orogenic interpretation of the Lewisian of Scotland. 23rd International
633 Geological Congress. 225-236.
- 634 Chapman, H. J., Moorbath, S., 1977. Lead isotope measurements from the oldest recognised Lewisian
635 gneisses of north-west Scotland. *Nature* 268, 41-42.
- 636 Cohen, A. S., O'Nions, R. K., O'Hara, M. J., 1991. Chronology and mechanism of depletion in
637 Lewisian granulites *Contributions to Mineralogy and Petrology* 106, 142-153.
- 638 Corfu, F., Heaman, L. M., Rogers, G., 1994. Polymetamorphic evolution of the Lewisian complex,
639 NW Scotland, as recorded by U-Pb isotopic compositions of zircon, titanite and rutile.
640 *Contributions to Mineralogy and Petrology* 117, 215-228.
- 641 Coward, M. P., 1990. Shear zones at the Laxford front, NW Scotland and their significance in the
642 interpretation of lower crustal structure. *Journal of the Geological Society of London* 147,
643 279-286.
- 644 Daly, J. S., Balagansky, V. V., Timmerman, M. J., Whitehouse, M. J., 2006. The Lapland-Kola
645 orogen: Palaeoproterozoic collision and accretion of the northern Fennoscandian lithosphere.
646 *Geological Society of London Memoir* 32, 579-598.

- 647 Daly, J. S., Muir, R. J., Cliff, R. A., 1991. A precise U-Pb zircon age for the Inishtrahull syenitic
648 gneiss, County Donegal, Ireland. *Journal of the Geological Society of London* 148, 639-642.
- 649 Davies, F. B., 1974. A layered basic complex in the Lewisian, south of Loch Laxford, Sutherland.
650 *Journal of the Geological Society of London* 130, 279-284.
- 651 Davies, F. B., 1976. Early Scourian structures in the Scourie-Laxford region and their bearing on the
652 evolution of the Laxford Front. *Journal of the Geological Society of London* 132, 543-554.
- 653 Evans, C. R., 1965. Geochronology of the Lewisian basement near Lochinver, Sutherland. *Nature*
654 207, 54-56.
- 655 Evans, C. R., Lambert, R. S. J., 1974. The Lewisian of Lochinver, Sutherland: the type area for the
656 Inverian metamorphism. *Journal of the Geological Society of London* 130, 125-150.
- 657 Friend, C. R. L., Kinny, P. D., 1995. New evidence for protolith ages of Lewisian granulites,
658 northwest Scotland. *Geology* 23, 1027-1030.
- 659 Friend, C. R. L., Kinny, P. D., 2001. A reappraisal of the Lewisian Gneiss Complex: geochronological
660 evidence for its tectonic assembly from disparate terranes in the Proterozoic. *Contributions to*
661 *Mineralogy and Petrology* 142, 198-218.
- 662 Garde, A. A., Chadwick, B., Grocott, J., Hamilton, M. A., McCaffrey, K. J., Swager, C. P., 2002b.
663 Mid-crustal partitioning and attachment during oblique convergence in an arc system,
664 Palaeoproterozoic Ketilidian orogen, southern Greenland *Journal of the Geological Society of*
665 *London* 159, 247-261.
- 666 Garde, A. A., Hamilton, M. A., Chadwick, B., Grocott, J., McCaffrey, K. J., 2002a. The Ketilidian
667 orogen of South Greenland: geochronology, tectonics, magmatism, and fore-arc accretion
668 during Palaeoproterozoic oblique convergence *Canadian Journal of Earth Sciences* 39, 765-
669 793.
- 670 Giletti, B. J., Moorbath, S., Lambert, R. S. J., 1961. A geochronological study of the metamorphic
671 complexes of the Scottish Highlands. *Quarterly Journal of the Geological Society of London*
672 117, 233-264.
- 673 Goodenough, K. M., Park, R. G., Krabbendam, M., Myers, J. S., Wheeler, J., Loughlin, S., Crowley,
674 Q., L., F. C. R., Beach, A., Kinny, P. D., Graham, R., 2010. The Laxford Shear Zone: an end-
675 Archaean terrane boundary? In: Law, R., Butler, R. W. H., Holdsworth, R. E., Krabbendam,
676 M., Strachan, R. (eds.), *Continental Tectonics and Mountain Building*. Geological Society
677 Special Publication 335. London: The Geological Society.
- 678 Hamilton, P. J., Evensen, N. M., O'Nions, R. K., Tarney, J., 1979. Sm-Nd systematics of Lewisian
679 gneisses: implications for the origin of granulites. *Nature* 277, 25-28.
- 680 Heaman, L., Tarney, J., 1989. U-Pb baddeleyite ages for the Scourie dyke swarm, Scotland: evidence
681 for two distinct intrusion events. *Nature, London* 340, 705-708.
- 682 Holmes, A., Shillibeer, H. A., Wilson, J. T., 1955. Potassium-Argon Ages of Some Lewisian and
683 Fennoscandian Pegmatites. *Nature* 176, 390-392.
- 684 Jackson, S. E., Pearson, N. J., Griffin, W. L., Belousova, E., 2004. The application of laser ablation
685 inductively coupled plasma mass spectrometry to in-situ U-Pb zircon geochronology.
686 *Chemical Geology* 211, 47-69.
- 687 Johnson, T. E., Fischer, S., White, R. W., Brown, M., Rollinson, H. R., 2012. Archaean Intracrustal
688 Differentiation from Partial Melting of Metagabbro - Field and Geochemical Evidence from
689 the Central Region of the Lewisian Complex, NW Scotland. *Journal of Petrology* 53, 2115-
690 2138.
- 691 Kalsbeek, F., Nutman, A. P., 1996. Anatomy of the Early Proterozoic Nagsugtoqidian orogen, West
692 Greenland, explored by reconnaissance SHRIMP U-Pb zircon dating. *Geology* 24, 515-518.
- 693 Kinny, P., Friend, C., 1997. U-Pb isotopic evidence for the accretion of different crustal blocks to form
694 the Lewisian Complex of Northwest Scotland. *Contributions to Mineralogy and Petrology*.
- 695 Kinny, P. D., Friend, C. R. L., J. L. G., 2005. Proposal for a terrane-based nomenclature for the
696 Lewisian Complex of NW Scotland. *Journal of the Geological Society of London* 162, 175-
697 186.
- 698 Lahtinen, R., Korja, A., Nironen, M., Heikkinen, P., 2009. Palaeoproterozoic accretionary processes in
699 Fennoscandia. In: Cawood, P. A., Kroner, A. (eds.), *Earth Accretionary Systems in Space and*
700 *Time*. Geological Society Special Publication 318. London: Geological Society, London.

- 701 Lambert, R. S. J., Holland, J. G., 1972. A geochronological study of the Lewisian from Loch Laxford
702 to Durness, Sutherland, N W Scotland. *Journal of the Geological Society of London* 128, 3-
703 19.
- 704 Love, G. J., Friend, C. R. L., Kinny, P. D., 2010. Palaeoproterozoic terrane assembly in the Lewisian
705 Gneiss Complex on the Scottish mainland, south of Gruinard Bay: SHRIMP U–Pb zircon
706 evidence. *Precambrian Research* 183, 89-111.
- 707 Love, G. J., Kinny, P., Friend, C. R. L., 2004. Timing of magmatism and metamorphism in the
708 Gruinard Bay area of the Lewisian Gneiss Complex: comparisons with the Assynt Terrane
709 and implications for terrane accretion *Contributions to Mineralogy and Petrology* 146, 620-
710 636.
- 711 Ludwig, K. R., 1980. Calculation of uncertainties of U-Pb isotope Data. *Earth and Planetary Science*
712 *Letters* 46, 212-220.
- 713 Ludwig, K. R., 1993. Pbdatt: a computer program for processing Pb-U-Th isotope data. *United States*
714 *Geological Survey, Open file reports*. 88-542, 1-34.
- 715 Ludwig, K. R., 2003. Isoplot 3.00: A geochronological toolkit for Microsoft Excel. *Berkeley*
716 *Geochronology Centre Special Publication* 4, 0-71.
- 717 Marcantonio, F., Dickin, A. P., McNutt, R. H., Heaman, L. M., 1988. A 1,800-million-year-old
718 Proterozoic gneiss terrane in Islay with implications for the crustal structure and evolution of
719 Britain. *Nature* 335, 62-64.
- 720 Mason, A. J., 2012. Major early thrusting as a control on the Palaeoproterozoic evolution of the
721 Lewisian Complex: evidence from the Outer Hebrides, NW Scotland. *Journal of the*
722 *Geological Society of London* 169, 201-212.
- 723 Mason, A. J., Brewer, T. S., 2005. A re-evaluation of a Laxfordian terrane boundary in the Lewisian
724 Complex of South Harris, NW Scotland. *Journal of the Geological Society of London* 162,
725 401-408.
- 726 Mason, A. J., Parrish, R. R., Brewer, T. S., 2004. U–Pb geochronology of Lewisian orthogneisses in
727 the Outer Hebrides, Scotland: implications for the tectonic setting and correlation of the South
728 Harris Complex *Journal of the Geological Society of London* 2004, 45-54.
- 729 Mattinson, J. M., 2005. Zircon U-Pb chemical abrasion ("CA-TIMS") method: Combined annealing
730 and multi-step partial dissolution analysis for improved precision and accuracy of zircon ages.
731 *Chemical Geology* 220, 47-66.
- 732 McAteer, C. A., Daly, J. S., Flowerdew, M. J., Connelly, J. N., Housh, T. B., Whitehouse, M. J., 2010.
733 Detrital zircon, detrital titanite and igneous clast U–Pb geochronology and basement–cover
734 relationships of the Colonsay Group, SW Scotland: Laurentian provenance and correlation
735 with the Neoproterozoic Dalradian Supergroup. *Precambrian Research* 181, 21-42.
- 736 Moorbath, S., Welke, H., Gale, N., 1969. The significance of lead isotope studies in ancient, high-
737 grade metamorphic basement complexes, as exemplified by the Lewisian rocks of Northwest
738 Scotland *Earth and Planetary Science Letters* 6, 245-256.
- 739 Mundil, R., Ludwig, K. R., Metcalfe, I., Renne, P. R., 2004. Age and timing of the Permian mass
740 extinctions: U-Pb dating of closed-system zircons *Science* 305, 1760-1763.
- 741 Nutman, A. P., Kalsbeek, F., Friend, C. R. L., 2008. The Nagssugtoqidian orogen in South-East
742 Greenland: Evidence for Paleoproterozoic collision and plate assembly. *American Journal of*
743 *Science* 308, 529-572.
- 744 Park, R. G., 1970. Observations on Lewisian chronology. *Scottish Journal of Geology* 6, 379-399.
- 745 Park, R. G., 1995. Palaeoproterozoic Laurentia-Baltica relationships: a view from the Lewisian. In:
746 Coward, M. P., Ries, A. C. (eds.), *Early Precambrian Processes*. Geological Society Special
747 Publication 95. London: The Geological Society.
- 748 Park, R. G., 2005. The Lewisian terrane model: a review. *Scottish Journal of Geology* 41, 105-118.
- 749 Park, R. G., Tarney, J., 1987. The Lewisian complex: a typical Precambrian high-grade terrain? In:
750 Park, R. G., Tarney, J. (eds.), *Evolution of the Lewisian and Comparable Precambrian High*
751 *Grade Terrains*. 27. London: Geological Society of London Special Publication.
- 752 Park, R. G., Tarney, J., Connelly, J. N., 2001. The Loch Maree Group: Palaeoproterozoic subduction–
753 accretion complex in the Lewisian of NW Scotland. *Precambrian Research* 105, 205-226.

- 754 Peach, B. N., Horne, J., Gunn, W., Clough, C. T., Hinxman, L. W., Teall, J. J. H., 1907. *The*
755 *geological structure of the North-West Highlands of Scotland*, Memoir of the Geological
756 Survey of Great Britain.
- 757 Pidgeon, R. T., Bowes, D. R., 1972. Zircon U–Pb ages of granulites from the Central Region of the
758 Lewisian, northwestern Scotland. *Geological Magazine* 109, 247-258.
- 759 Rogers, J. J. W., Santosh, M., 2002. Configuration of Columbia, a Mesoproterozoic Supercontinent.
760 *Gondwana Research* 5, 5-22.
- 761 Rollinson, H. R., Windley, B. F., 1980. Geochemistry and origin of an Archaean granulite grade
762 tonalite-trondhjemite-granite suite from Scourie, NW Scotland. *Contributions to Mineralogy*
763 *and Petrology* 72, 265-281.
- 764 Scott, D. J., 1998. An overview of the U-Pb geochronology of the Paleoproterozoic Torngat Orogen,
765 Northeastern Canada. *Precambrian Research* 91, 91-107.
- 766 St-Onge, M. R., van Gool, J. A. M., Garde, A. A., Scott, D. J., 2009. Correlation of Archaean and
767 Palaeoproterozoic units between northeastern Canada and western Greenland: constraining
768 the pre-collisional upper plate accretionary history of the Trans-Hudson orogen. In: Cawood,
769 P. A., Kroner, A. (eds.), *Earth Accretionary Systems in Space and Time*. Geological Society
770 Special Publication 318. London: The Geological Society, London.
- 771 Stacey, J. S., Kramer, J. D., 1975. Approximation of terrestrial lead isotope evolution by a two stage
772 model. *Earth and Planetary Science Letters* 26, 207-221.
- 773 Sutton, J., Watson, J. V., 1951. The pre-Torridonian metamorphic history of the Loch Torridon and
774 Scourie areas in the northwest Highlands, and its bearing on the chronological classification
775 of the Lewisian. *Quarterly Journal of the Geological Society of London* 106, 241-307.
- 776 Tarney, J., Weaver, B. L., 1987. Geochemistry of the Scourian complex: petrogenesis and tectonic
777 models. In: Park, R. G., Tarney, J. (eds.), *Evolution of the Lewisian and Comparable*
778 *Precambrian High Grade Terrains*. Geological Society of London Special Publication 27.
779 London: Geological Society of London.
- 780 Thomas, R. J., Jacobs, J., Horstwood, M. S. A., Ueda, K., Bingen, B., Matola, R., 2010. The Mecubúri
781 and Alto Benfica Groups, NE Mozambique: aids to unravelling ca.1 Ga and 0.5 Ga events in
782 the East African Orogen. *Precambrian Research* 178, 72-90.
- 783 van Gool, J. A. M., Connelly, J. N., Marker, M., Mengel, F. C., 2002. The Nagssugtoqidian Orogen of
784 West Greenland: tectonic evolution and regional correlations from a West Greenland
785 perspective *Canadian Journal of Earth Sciences* 39, 665-686.
- 786 van Kranendonk, M. J., St-Onge, M. R., Henderson, J. R., 1993. Paleoproterozoic tectonic assembly of
787 Northeast Laurentia through multiple indentations. *Precambrian Research* 63, 325-347.
- 788 Watkins, J. M., Clemens, J. D., Treloar, P. J., 2007. Archean TTGs as sources of younger granitic
789 magmas: melting of sodic metatonalites at 0.6-1.2 GPa. *Contributions to Mineralogy and*
790 *Petrology* 154, 91-110.
- 791 Wheeler, J., Park, R. G., Rollinson, H. R., Beach, A., 2010. The Lewisian Complex: insights into deep
792 crustal evolution. In: Law, R., Butler, R. W. H., Holdsworth, R. E., Krabbendam,
793 M., Strachan, R. (eds.), *Continental Tectonics and Mountain Building: the Legacy of Peach*
794 *and Horne*. Geological Society Special Publication 335. London: The Geological Society.
- 795 Whitehouse, M. J., 1989. Sm-Nd evidence for diachronous crustal accretion in the Lewisian complex
796 of northwest Scotland. *Tectonophysics* 161, 245-256.
- 797 Whitehouse, M. J., 1990. An early-Proterozoic age for the Ness anorthosite, Lewis, Outer Hebrides.
798 *Scottish Journal of Geology* 26, 131-136.
- 799 Whitehouse, M. J., Bridgwater, D., 2001. Geochronological constraints on Paleoproterozoic crustal
800 evolution and regional correlations of the northern Outer Hebridean Lewisian complex,
801 Scotland. *Precambrian Research* 105, 227-245.
- 802 Whitehouse, M. J., Kemp, A. I. S., 2010. On the difficulty of assigning crustal residence, magmatic
803 protolith and metamorphic ages to Lewisian granulites: constraints from combined in situ U-
804 Pb and Lu-Hf isotopes. In: Law, R., Butler, R. W. H., Holdsworth, R. E., Krabbendam,
805 M., Strachan, R. (eds.), *Continental Tectonics and Mountain Building: the Legacy of Peach*
806 *and Horne*. Geological Society Special Publication 335. London: Geological Society of
807 London.

808 Whitehouse, M. J., Moorbath, S., 1986. Pb–Pb systematics of Lewisian gneisses—implications for
809 crustal differentiation. *Nature* 319, 488-489.
810 Zhao, G., Sun, M., Wilde, S. A., Li, S., 2004. A Paleo-Mesoproterozoic supercontinent: assembly,
811 growth and breakup. *Earth Science Reviews* 67, 91-123.
812 Zhu, X. K., O'Nions, R. K., Belshaw, N. S., Gibb, A. J., 1997. Lewisian crustal history from in situ
813 SIMS mineral chronometry and related metamorphic textures. *Chemical Geology* 136, 205-
814 218.
815 Zirkler, A., Johnson, T. E., White, R. W., Zack, T., 2012. Polymetamorphism in the mainland
816 Lewisian complex, NW Scotland - phase equilibria and geochronological constraints from the
817 Cnoc an t'Sidhean suite. *Journal of Metamorphic Geology* 30, 865-885.

818

819 **Figure captions**

- 820 1. Generalised map of the Lewisian Gneiss Complex in Northwest Scotland, showing
821 the main structural features, after Kinny et al. (2005) and Wheeler et al. (2010).
- 822 2. Simplified geological map of the Laxford Shear Zone, after Goodenough et al.
823 (2010). Sample localities: 1, Badnabay; 2, Tarbet; 3, Ben Stack; 4, Rhiconich
- 824 3. a) Photograph of the Tarbet locality, showing granite sheets that have been tightly
825 folded by Inverian deformation; sample LX11 was collected from one of these
826 granite sheets. c. 80 cm sledgehammer for scale. b) Photograph of the Rhiconich
827 locality, showing anastomosing, undeformed granite sheets; sample LX7 was
828 collected from one of these.
- 829 4. Representative CL images of zircon grains from the dated samples LX1, LX2, LX6,
830 LX7, and LX11.
- 831 5. Concordia plots for samples from Badnabay and Tarbet. a) U-Pb zircon ID-TIMS
832 data for sample LX1; b) U-Pb zircon LA-ICPMS data for sample LX1; c) U-Pb
833 zircon concordia diagram for sample LX2; d) U-Pb zircon concordia diagram for
834 sample LX11. All data-point error ellipses are 2σ .
- 835 6. Concordia plots for samples from Ben Stack and Rhiconich. a) U-Pb concordia
836 diagram for all data from sample LX6, b) probability plot showing $^{207}\text{Pb}/^{206}\text{Pb}$ age

837 for sample LX6, c) U-Pb concordia diagram of c. 1880 Ma population from LX6;
838 d) Tera Wasserburg diagram for sample LX6 titanites; e) U-Pb zircon concordia
839 diagram for all data from sample LX7; f) U-Pb zircon concordia diagram for c.
840 1790 Ma cluster from sample LX7. All data-point error ellipses are 2σ .

841

842 **Tables (may be published as supplementary data if necessary)**

- 843 1. LA-ICPMS U-Pb data for zircon from LX1
- 844 2. TIMS U-Pb data for zircon from LX1
- 845 3. LA-ICPMS data for zircon from LX2
- 846 4. LA-ICPMS data for zircon from LX11
- 847 5. LA-ICPMS data for zircon from LX6
- 848 6. LA-ICPMS data for titanite from LX6
- 849 7. LA-ICPMS data for zircon from LX7
- 850 8. Summary of the dates for the Lewisian Gneiss Complex presented in this paper.

851

Analysis	Concentrations (ppm)					†Ratios						Ages (Ma)						% disc	
	(mV)		²³⁸ U	Pb	U*	²⁰⁷ Pb/ ²⁰⁶ Pb	±1s %	²⁰⁶ Pb/ ²³⁸ U	±1s %	²⁰⁷ Pb/ ²³⁵ U	±1s %	Rho	²⁰⁷ Pb/ ²⁰⁶ Pb	±2s abs	²⁰⁶ Pb/ ²³⁸ U	±2s abs	²⁰⁷ Pb/ ²³⁵ U		±2s abs
LX-1_Z1_1	0.27	0.04																0.68	
LX-1_Z1_2	0.59	0.10	1.38	5	9	0.1867	1.0	0.5553	1.8	14.2974	2.1	0.86	2714	17	2847	128	2770	475	-5
LX-1_Z1_3	1.34	0.25	2.81	10	18	0.2050	0.7	0.6037	1.1	17.0669	1.3	0.83	2867	12	3045	82	2939	369	-6
LX-1_Z1_4	1.52	0.24	3.63	12	24	0.1789	0.7	0.5240	1.0	12.9268	1.2	0.83	2643	11	2716	69	2674	281	-3
LX-1_Z1_5	1.06	0.19	2.41	8	16	0.2003	0.7	0.5485	1.1	15.1487	1.3	0.83	2829	12	2819	75	2825	334	0
LX-1_Z2_1	8.67	0.85	33.51	67	217	0.1100	0.5	0.3298	0.9	5.0033	1.0	0.87	1800	9	1838	37	1820	97	-2
LX-1_Z2_2	11.61	1.14	46.06	90	298	0.1105	0.1	0.3264	0.9	4.9724	0.9	0.99	1807	2	1821	36	1815	84	-1
LX-1_Z2_3	4.16	0.41	16.15	32	104	0.1113	0.3	0.3179	0.9	4.8801	0.9	0.94	1822	6	1779	36	1799	90	2
LX-1_Z2_4	4.45	0.44	17.06	35	110	0.1107	0.5	0.3185	0.9	4.8619	1.0	0.87	1811	9	1782	37	1796	96	2
LX-1_Z2_5	12.89	1.76	37.21	100	241	0.1531	1.0	0.4210	1.1	8.8885	1.4	0.74	2381	17	2265	58	2327	233	5
LX-1_Z2_6	6.60	0.65	24.40	51	158	0.1109	0.5	0.3342	0.9	5.1106	1.1	0.88	1815	9	1859	40	1838	105	-2
LX-1_Z3_1	3.89	0.45	13.32	30	86	0.1305	0.3	0.3700	1.0	6.6585	1.0	0.95	2105	6	2029	46	2067	130	4
LX-1_Z3_2	3.39	0.36	12.45	26	81	0.1202	0.4	0.3485	0.9	5.7738	1.0	0.91	1959	7	1927	42	1942	115	2
LX-1_Z3_3	4.48	0.54	14.76	35	96	0.1350	0.3	0.3879	1.0	7.2232	1.0	0.95	2165	5	2113	49	2139	140	2
LX-1_Z4_1	12.14	1.86	32.52	94	210	0.1725	0.3	0.4745	1.1	11.2836	1.1	0.96	2582	5	2503	64	2547	224	3
LX-1_Z5_1	4.27	0.41	16.81	33	109	0.1079	0.3	0.3263	1.0	4.8532	1.0	0.96	1764	6	1821	41	1794	97	-3
LX-1_Z5_2	3.47	0.34	13.20	27	85	0.1106	0.4	0.3203	0.8	4.8831	0.9	0.92	1809	7	1791	35	1799	88	1
LX-1_Z5_3	1.73	0.17	6.46	13	42	0.1103	0.6	0.3279	0.9	4.9860	1.1	0.84	1804	11	1828	39	1817	105	-1
LX-1_Z5_4	1.09	0.11	3.95	8	26	0.1110	0.5	0.3400	1.1	5.2026	1.2	0.91	1816	9	1886	47	1853	119	-4
LX-1_Z6_1	4.50	0.44	17.58	35	114	0.1088	0.3	0.3301	1.0	4.9495	1.0	0.96	1779	6	1839	42	1811	100	-3
LX-1_Z6_2	2.91	0.28	11.17	23	72	0.1087	0.4	0.3130	0.8	4.6917	0.9	0.90	1778	7	1755	33	1766	83	1
LX-1_Z6_3	1.70	0.17	6.22	13	40	0.1097	0.5	0.3322	0.8	5.0252	1.0	0.86	1795	9	1849	36	1824	96	-3
LX-1_Z7_1	13.79	2.11	37.81	107	245	0.1730	0.1	0.4724	1.0	11.2682	1.0	0.99	2587	2	2494	61	2546	208	4
LX-1_Z8_1	4.93	0.48	19.23	38	124	0.1083	0.3	0.3291	0.9	4.9134	0.9	0.96	1770	5	1834	37	1805	88	-4
LX-1_Z8_2	1.98	0.19	7.36	15	48	0.1108	0.5	0.3247	0.8	4.9600	1.0	0.86	1813	9	1812	35	1813	93	0
LX-1_Z8_3	1.23	0.12	4.41	10	29	0.1106	0.5	0.3348	1.0	5.1036	1.1	0.89	1808	9	1862	42	1837	108	-3
LX-1_Z8_4	1.80	0.18	6.74	14	44	0.1100	0.6	0.3246	0.8	4.9221	1.0	0.81	1799	11	1812	34	1806	97	-1
LX-1_Z9_1	15.72	2.55	39.87	122	258	0.1820	0.2	0.5032	0.9	12.6310	1.0	0.97	2672	4	2628	61	2653	223	2
LX-1_Z10_1	7.06	0.68	28.12	55	182	0.1084	0.2	0.3240	0.8	4.8438	0.9	0.97	1773	4	1809	35	1793	82	-2
LX-1_Z10_2	7.02	0.68	27.71	54	179	0.1078	0.2	0.3270	0.9	4.8619	0.9	0.97	1763	4	1824	37	1796	86	-3
LX-1_Z10_3	4.22	0.41	14.74	33	95	0.1091	0.3	0.3357	0.8	5.0490	0.9	0.94	1784	6	1866	36	1828	88	-5
LX-1_Z10_4	4.33	0.42	16.12	34	104	0.1094	0.5	0.3211	0.8	4.8432	1.0	0.86	1789	9	1795	35	1792	92	0
LX-1_Z10_5	4.35	0.43	16.27	34	105	0.1098	0.3	0.3205	0.8	4.8533	0.9	0.94	1797	5	1792	35	1794	84	0
LX-1_Z10_6	4.15	0.40	14.91	32	96	0.1091	0.4	0.3334	1.0	5.0139	1.1	0.94	1784	6	1855	43	1822	104	-4
LX-1_Z10_7	4.27	0.42	16.06	33	104	0.1110	0.3	0.3197	0.9	4.8922	1.0	0.96	1816	5	1788	39	1801	93	2

*Accuracy of U concentration is c.20%

†Isotope ratios are not common Pb corrected

§% Discordance is measured as ²⁰⁶Pb/²³⁸U age relative to ²⁰⁷Pb/²⁰⁶Pb age

	weight (μg)	U(ppm)	Pb(ppm) [†]	Pb (pg) [‡]	Th/U	Isotopic ratios						Ages (Ma)							
						²⁰⁶ Pb/ ²⁰⁴ Pb [§]	²⁰⁷ Pb/ ²⁰⁶ Pb [¶]	2 σ (%)	²⁰⁶ Pb/ ²³⁸ U ^{¶¶}	2 σ (%)	²⁰⁷ Pb/ ²³⁵ U ^{¶¶}	2 σ (%)	Rho ^{¶¶}	²⁰⁷ Pb/ ²⁰⁶ Pb	2 σ (Ma)	²⁰⁶ Pb/ ²³⁸ U	2 σ (Ma)	²⁰⁷ Pb/ ²³⁵ U	2 σ (Ma)
LX-1																			
Z1	0.1	684.6	249.6	1.3	0.8	1081.1	0.10843	0.12	0.31644	0.19	4.73093	0.23	0.85	1773.3	2.2	1772.3	3.3	1772.7	4.0
Z2	0.2	442.3	148.8	1.7	0.4	1044.7	0.10835	0.12	0.31572	0.27	4.71683	0.30	0.91	1771.9	2.2	1768.8	4.7	1770.2	5.2
Z3	0.5	470.2	192.2	2.6	1.3	1664.3	0.10810	0.16	0.30922	0.18	4.60888	0.24	0.77	1767.6	2.8	1736.9	3.2	1750.9	4.3
Z4	0.2	510.8	206.0	2.2	1.1	919.4	0.10846	0.09	0.31582	0.23	4.72293	0.25	0.93	1773.7	1.7	1769.3	4.1	1771.3	4.5
Z5	0.3	96.4	43.7	2.1	0.9	303.9	0.12695	0.39	0.34218	0.73	5.98938	0.85	0.89	2056.1	6.9	1897.2	13.8	1974.3	16.7

*Samples not being subjected to ion-exchange procedures

[†]Radiogenic lead corrected for mass fractionation, laboratory Pb, spike and initial common Pb

[‡]Total common Pb

[§]²⁰⁶Pb/²⁰⁴Pb is a measured ratio corrected for mass fractionation and common lead in the ²⁰⁵Pb/²³⁵U spike

[¶]Corrected for mass fractionation, laboratory Pb & U spike and initial common Pb

^{¶¶}Error correlation coefficient calculated using isoplot (Ludwig, 2003)

Analysis	Concentration (mV)			Concentration (ppm)		†Ratios						Ages (Ma)						% disc	
	²⁰⁶ Pb	²⁰⁷ Pb	²³⁸ U	Pb	U*	²⁰⁷ Pb/ ²⁰⁶ Pb	±1s %	²⁰⁶ Pb/ ²³⁸ U	±1s %	²⁰⁷ Pb/ ²³⁵ U	±1s %	Rho	²⁰⁷ Pb/ ²⁰⁶ Pb	±2s abs	²⁰⁶ Pb/ ²³⁸ U	±2s abs	²⁰⁷ Pb/ ²³⁵ U		±2s abs
LX7_Z1_1	7.02	1.06	18.40	50	109	0.1714	1.2	0.4707	1.4	11.1266	1.9	0.76	2572	21	2487	58	2534	34	3
LX7_Z1_2	13.10	2.23	31.40	93	185	0.1936	0.2	0.5327	0.9	14.2196	1.0	0.98	2773	3	2753	41	2764	18	1
LX7_Z1_3	8.30	1.45	19.39	59	115	0.1988	0.2	0.5378	1.6	14.7436	1.6	0.99	2817	3	2774	72	2799	30	2
LX7_Z2_1	6.85	0.66	26.97	48	159	0.1096	0.2	0.3238	0.9	4.8940	0.9	0.98	1793	4	1808	29	1801	16	-1
LX7_Z2_2	7.58	0.73	29.55	54	175	0.1096	0.2	0.3192	0.9	4.8220	0.9	0.98	1792	3	1786	28	1789	16	0
LX7_Z2_3	6.93	0.67	27.36	49	162	0.1098	0.2	0.3146	0.9	4.7622	0.9	0.98	1796	3	1764	28	1778	15	2
LX7_Z2_4	6.15	0.60	22.95	44	136	0.1101	0.2	0.3387	0.9	5.1405	0.9	0.97	1801	4	1880	28	1843	15	-4
LX7_Z3_1	8.69	1.35	23.06	61	136	0.1775	0.3	0.4768	1.0	11.6676	1.0	0.95	2629	5	2514	40	2578	19	4
LX7_Z3_2	8.10	1.40	18.25	57	108	0.1971	0.1	0.5587	0.8	15.1803	0.9	0.99	2802	2	2861	39	2827	16	-2
LX7_Z3_3	5.20	0.90	11.50	37	68	0.1991	0.2	0.5654	1.1	15.5238	1.1	0.99	2819	3	2889	49	2848	20	-2
LX7_Z4_1	11.43	1.12	41.72	81	246	0.1116	0.2	0.3474	0.9	5.3455	0.9	0.98	1826	3	1922	29	1876	15	-5
LX7_Z4_2	9.35	1.00	33.52	66	198	0.1212	0.7	0.3507	1.1	5.8611	1.3	0.84	1974	13	1938	38	1955	23	2
LX7_Z5_1	9.69	1.51	24.13	69	142	0.1778	0.4	0.5220	0.9	12.7945	1.0	0.94	2632	6	2708	41	2665	19	-3
LX7_Z6_1	9.16	0.88	35.58	65	210	0.1095	0.2	0.3260	0.9	4.9223	0.9	0.98	1791	3	1819	27	1806	15	-2
LX7_Z7_1	14.32	1.40	55.45	101	328	0.1112	0.3	0.3300	0.9	5.0588	1.0	0.97	1819	5	1838	30	1829	16	-1
LX7_Z8_1	2.52	0.41	6.46	18	38	0.1851	0.3	0.4997	1.0	12.7542	1.1	0.95	2699	5	2612	43	2662	20	3
LX7_Z8_2	2.68	0.46	6.18	19	36	0.1956	0.3	0.5543	0.9	14.9495	0.9	0.96	2790	4	2843	40	2812	17	-2
LX7_Z10_1	6.83	0.67	25.41	48	150	0.1114	0.3	0.3408	0.9	5.2325	0.9	0.95	1822	5	1891	28	1858	15	-4
LX7_Z11_1	6.84	1.16	16.35	48	97	0.1924	0.2	0.5308	0.9	14.0819	0.9	0.98	2763	3	2745	39	2755	17	1
LX7_Z12_1	9.89	1.65	23.25	70	137	0.1898	0.1	0.5345	1.0	13.9872	1.1	0.99	2740	2	2760	47	2749	20	-1
LX7_Z13	12.18	2.01	27.81	95	176	0.1876	0.3	0.5551	0.9	14.3545	1.0	0.95	2721	5	2846	41	2773	18	-5
LX7_Z15	12.67	2.12	29.82	90	176	0.1900	0.1	0.5438	0.8	14.2447	0.8	0.99	2742	2	2799	38	2766	16	-2
LX7_Z17	6.45	1.17	14.34	46	85	0.2049	0.2	0.5700	1.0	16.0982	1.0	0.98	2865	3	2908	48	2883	20	-1
LX7_Z18	10.74	1.43	32.81	76	194	0.1510	0.2	0.4148	0.9	8.6358	0.9	0.98	2357	3	2237	32	2300	16	5
LX7_Z19	9.07	0.87	35.34	64	209	0.1088	0.2	0.3234	0.9	4.8522	0.9	0.98	1780	3	1806	28	1794	15	-1
LX7_Z20	13.08	1.98	32.69	92	193	0.1709	0.6	0.5107	1.0	12.0333	1.2	0.83	2566	11	2660	42	2607	21	-4

*Accuracy of U concentration is c.20%

†Isotope ratios are not common Pb corrected

§% Discordance is measured as ²⁰⁶Pb/²³⁸U age relative to ²⁰⁷Pb/²⁰⁶Pb age

Table 8

Age (approx)	Locality	Sample number	Event
1670 Ma	Ben Stack	LX6	Post-Laxfordian cooling through titanite closure temperature (600-700 °C)
1750 Ma	Tarbet	LX11	Laxfordian metamorphism
1773 Ma	Badnabay	LX1	Granite emplacement during partial melting of local crust
1793 Ma	Rhiconich	LX7	Granite emplacement during partial melting of local crust
1880 Ma	Ben Stack	LX6	Alkaline granite intrusion
2475 Ma	Badnabay	LX2	Inverian metamorphism
2480 Ma	Tarbet	LX11	Partial melting and Inverian metamorphism
2840 Ma	Tarbet	LX11	Inherited country rock gneiss protolith age

Figure 1
[Click here to download high resolution image](#)

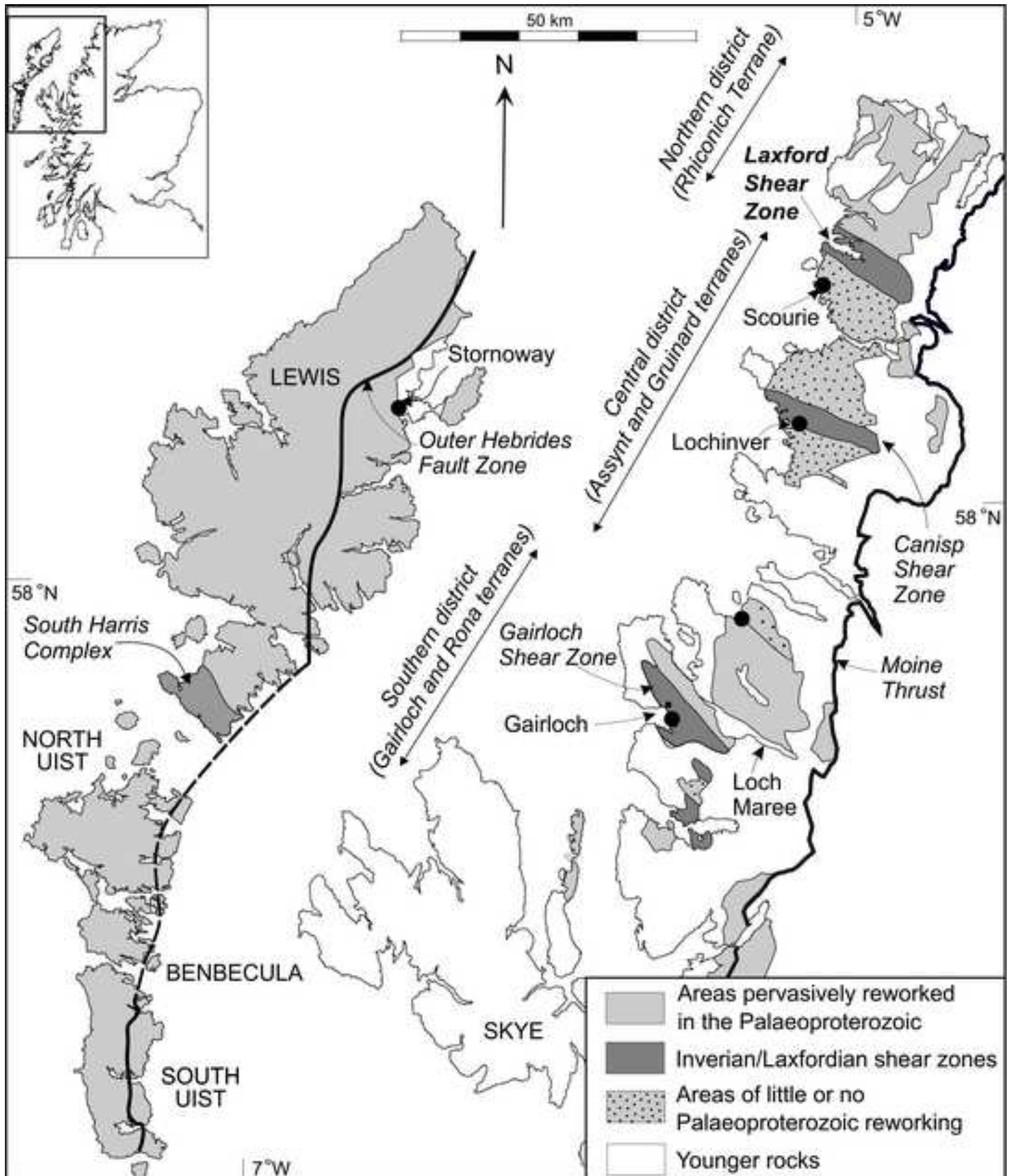


Figure 2
[Click here to download high resolution image](#)

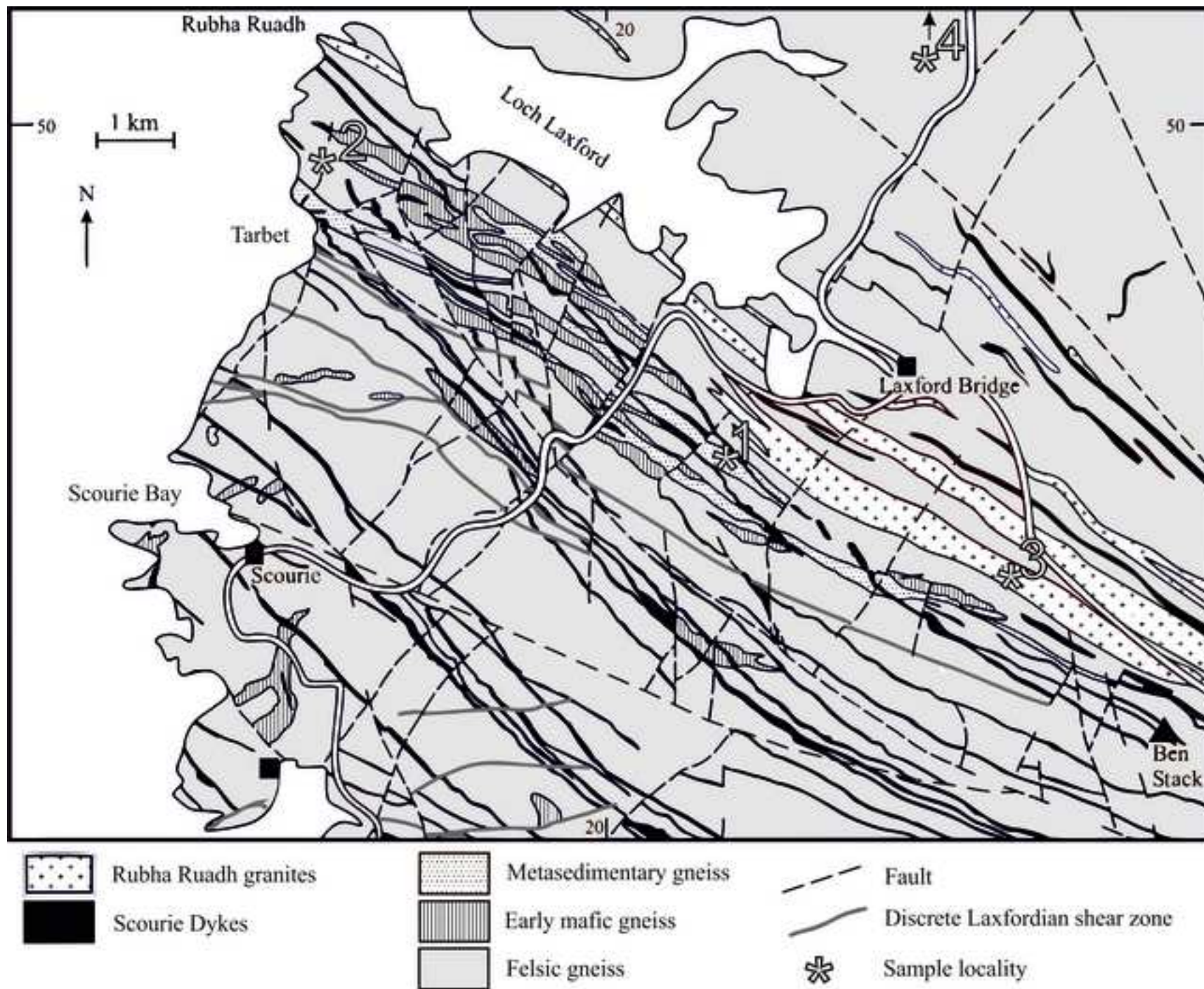


Figure 3
[Click here to download high resolution image](#)



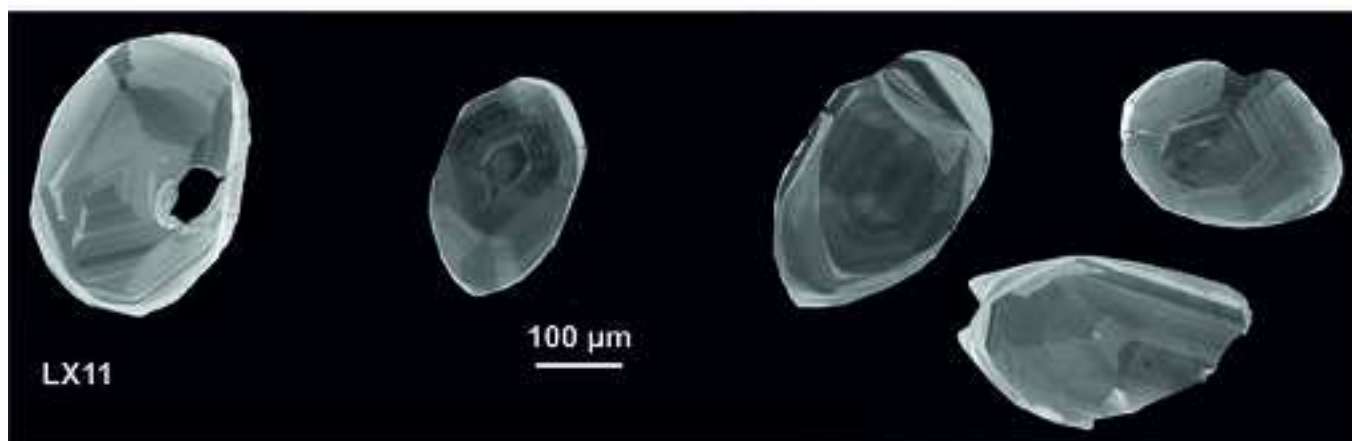
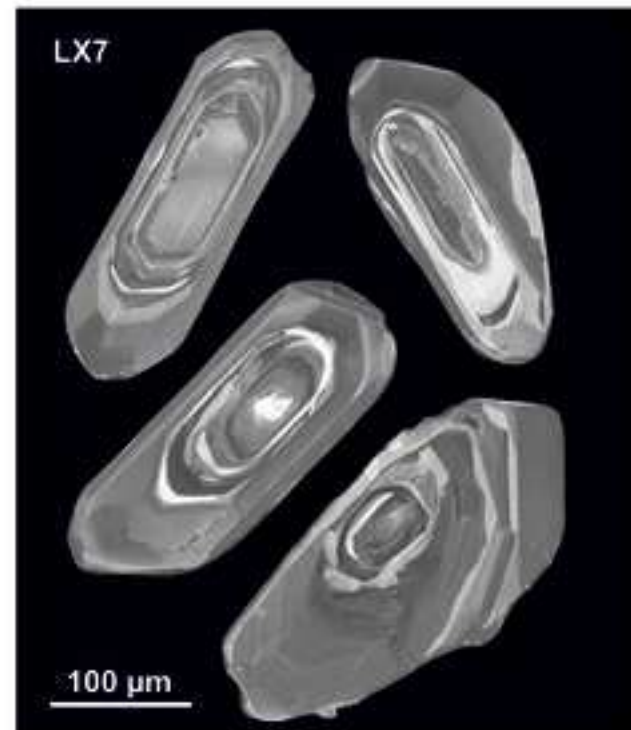
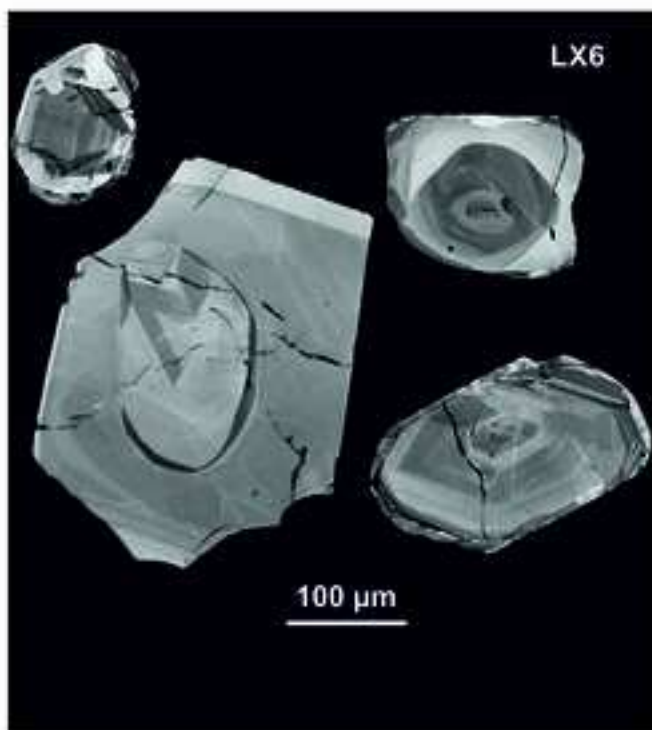
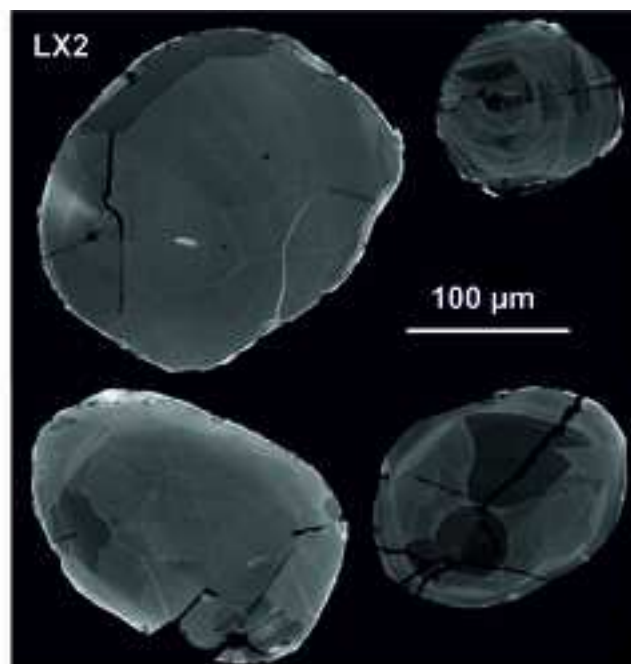
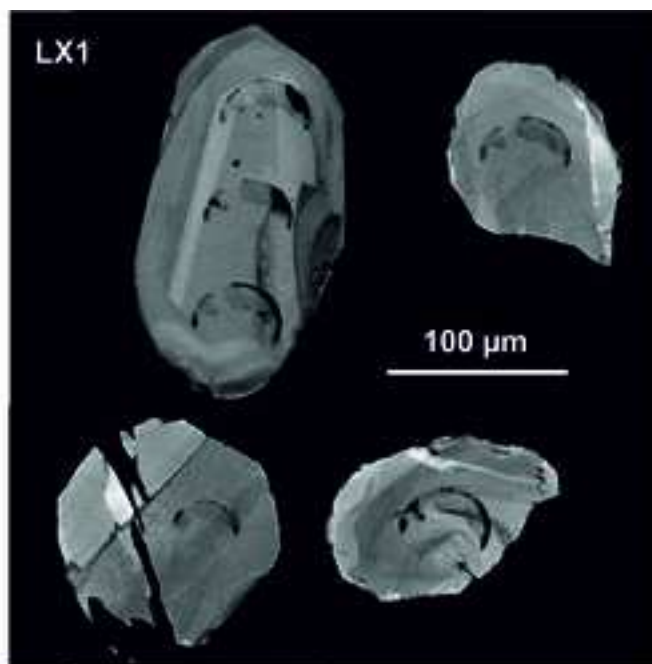


Figure5.jpg

[Click here to download high resolution image](#)

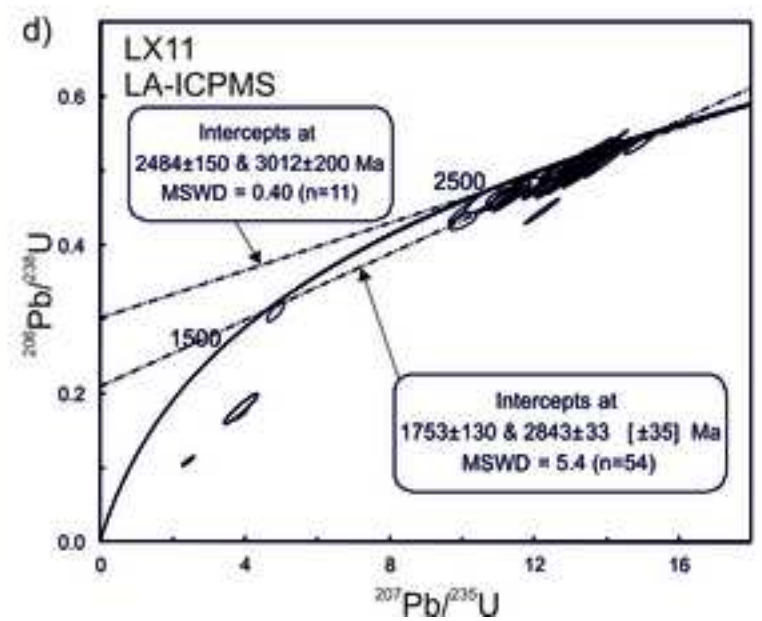
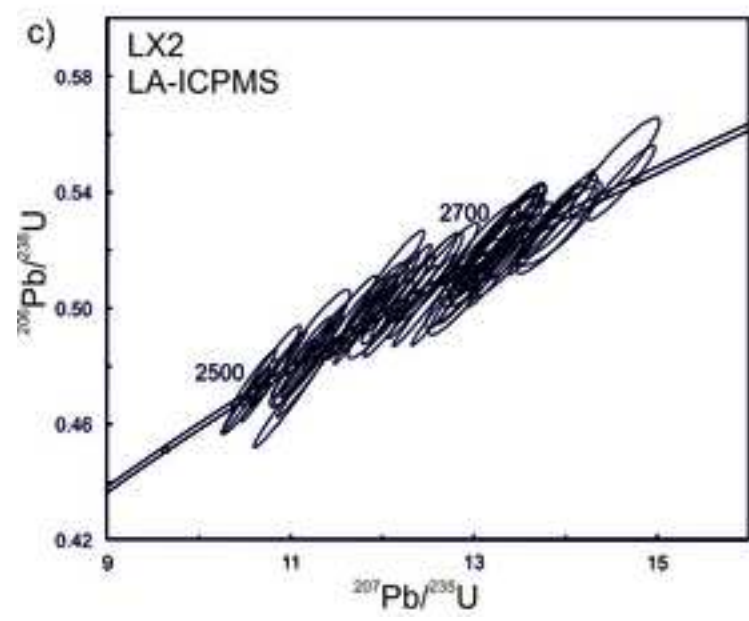
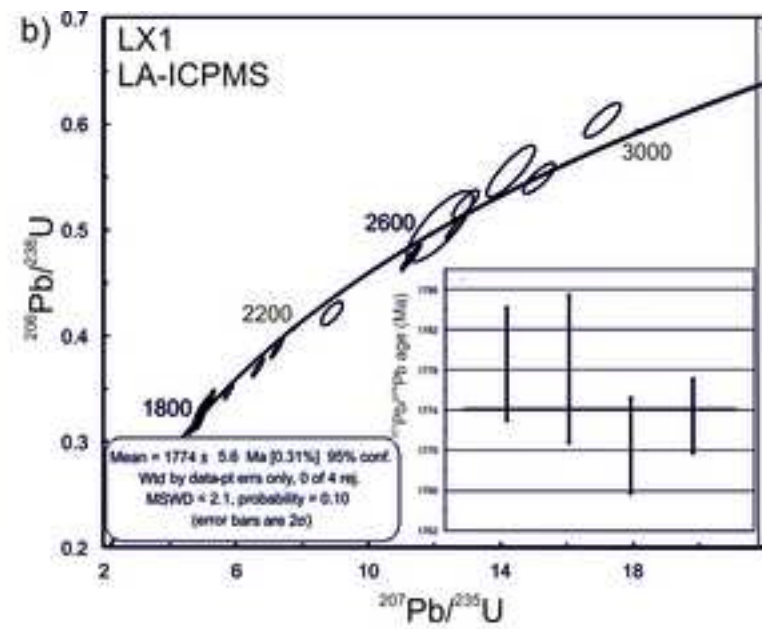
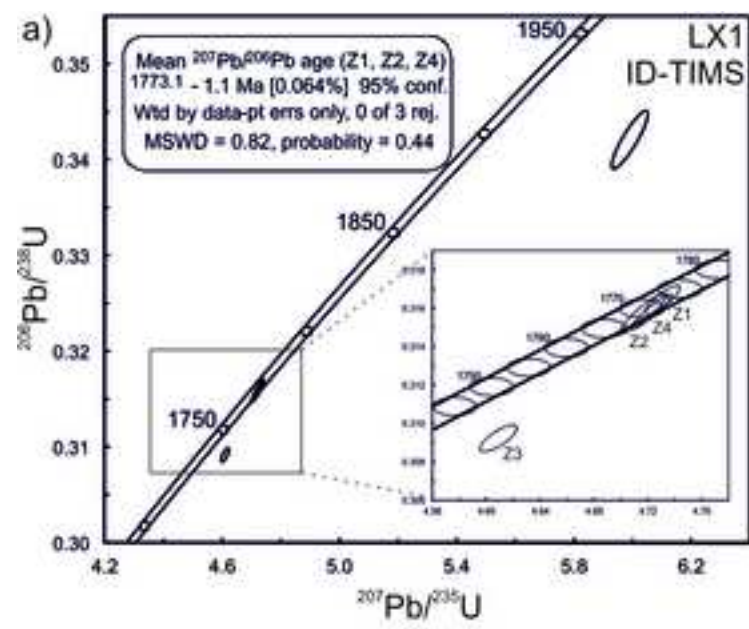


Figure6.jpg
[Click here to download high resolution image](#)

